PETROGRAPHIC ANALYSIS AND DIAGENETIC HISTORY OF THE VIOLA LIMESTONE AT STEPHEN'S RANCH, IN THE MORRISON NORTHEAST FIELD OF CLARK COUNTY, KANSAS

by

ARIA LINARES

B.S., University of Oklahoma, 2013

A THESIS

submitted in partial fulfillment of the requirements for the degree

MASTER OF SCIENCE

Department of Geology
College of Arts and Sciences

KANSAS STATE UNIVERSITY
Manhattan, Kansas

2016

Approved by:

Major Professor
Dr. Matthew Totten

Copyright

Abstract

The Viola Limestone is a prominent petroleum reservoir in the Mid-Continent Region, particularly in Oklahoma and Kansas. Coral Coast Petroleum established production from the Viola Ls. in 2011 in their Stephens Ranch lease in Clark County, south-central Kansas. Development of this lease has been hindered by the unpredictable production rates encountered in each of the subsequent eleven development wells. Infield drilling locations to date were chosen by favorable structural position as determined by 3D seismic. The best reservoir conditions, however, do not necessarily coincide with structural position. It was the purpose of this study to determine whether the ideal porosity and permeability are controlled by depositional environment, diagenetic alterations, or a combination of these factors.

Several approaches to solve this question were implemented and utilized, including well log analysis, petrographic inspection of well cuttings and thin sections, and the application of the Scanning Electron Microscope (SEM). An exploration model of the Viola Ls. in this field was developed, where the Viola A and B zones were dolomitized during during marine transgressions by mixing of sea water with other Mg-rich fluids. Reservoir conditions are found where these facies were preserved as paleotopographic highs during a subsequent sea level low-stand. These preserved dolomitized facies correspond to the seismic facies identified by seismic attributes in a 3D seismic study by Vohs (2016).

Table of Contents

List of Figures

List of Tables

Acknowledgements

I would like to express gratitude to my advisor, Dr. Matthew Totten, and my committee members, Dr. Abdelmoneam Raef and Dr. Sambhudas Chaudhuri, for offering guidance and encouragement in the fulfillment of my research. I would also like to sincerely thank Dr. Pamela Kempton, and other members of the geology department at Kansas State University, by providing generous support on the completion of my thesis. I am also appreciative of the well data provided by Coral Coast, LLC.

Dedication

I would like to dedicate this thesis to my family, as they have always nurtured and supported my goals and pursuits in the geosciences.

Chapter 1- Introduction to Carbonate Reservoirs

1.1 Introduction

The petroleum reservoir quality of a sedimentary rock is fundamentally controlled by the rock's petrophysical properties, such as porosity and permeability. These characteristics determine the amount of hydrocarbons that the reservoir can store, as well as the fluid flow properties within the reservoir rock (Cone and Kersey, 1992). The sedimentary process in its entirety helps steer and shape the various constituents of the sedimentary rock, but it is the rock's depositional environment and diagenetic processes that are responsible for the lithologic changes that occur at the onset of deposition (Syed et al., 2010). During deposition, the mechanical and chemical compaction imparted by diagenesis can permanently alter the textural fabric and structural components of the rock (Syed et al., 2010). These textural changes alter the nature of grain contacts within the rock, ultimately either inhibiting or enhancing the overall porosity and permeability (Cone and Kersey, 1992). For that reason, the reservoir quality is contingent on the mechanical and chemical reactions that transpire during and post-deposition (Syed et al., 2010).

The processes responsible for imparting porosity in clastic and carbonate reservoirs may differ significantly (Syed et al., 2010). For carbonate rocks, the depositional environment plays a key role in shaping the carbonate reservoir potential. Most carbonates are deposited *in situ* in a marine setting that is susceptible to precipitating moderately porous limestone or dolostone (Boggs and Krinsley, 2006). The following model depicts the environment in which carbonates typically precipitate (Figure 1-1).

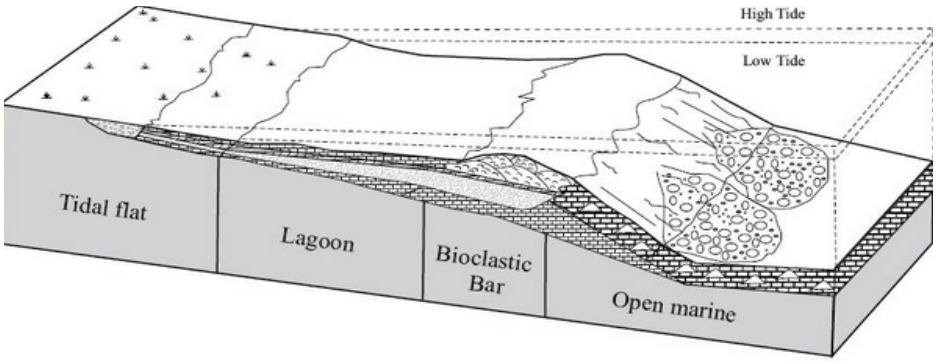

Figure 1-1. Model depositional environment of carbonate rocks (Vaziri et al., 2012).

Alongside the depositional environment, the process of diagenesis is also a fundamental constituent in the sedimentary process that contributes in the development of a carbonate rock's lithologic properties. The diagenetic process is the last stage that sediments undergo, beginning at the onset of deposition and ending with rock lithification (Syed et al., 2010). Throughout the post-depositional process of diagenesis, carbonate rocks are exposed to episodic phases of precipitation, pressure solution, dissolution, and cementation, which collectively is known as the paragenetic sequence (Boggs and Krinsley, 2006). These sequential stages of the diagenetic process result in the final, stable mineral assemblage within the rock's structural fabric (Bathurst, 1975).

The alterations exhibited in the skeletal allochems and textures within carbonate rocks form as a result of the mineralogical changes that ensue during burial (Syed et al., 2010). The textural pore groups that form are dependent on the chemical stability of the rock as it is being buried (Syed et al., 2010), and include the following (Figure 1-2): fabric selective, non-fabric selective, and either fabric selective or non-fabric selective (Longman, 1981). The pore types exhibited in the fabric selective group include textural frameworks in which the void space is present between grains or fossils (interparticle/fenestral) or within the grain or fossil (intraparticle), or can have void space present within the framework of carbonate structures (growth-framework) (Longman

1981; Murray and Pray, 1965). For the non-fabric selective group, the void space forms three distinct types of porosities: fracture, channel, and vuggy porosity (Longman, 1981). Void space that grows independent of the structural fabric can belong to either group and includes boring, burrowing, brecciation and shrinkage porosity (Longman, 1981). Although the structure of the different porosity groups is initially influenced by the depositional environment, the process of diagenesis contributes most of the framework alternations that take place among all of the porosity groups (Syed et al., 2010). The depositional environment and diagenesis acutely impact porosity growth throughout the various stages of burial and lithification, consequently developing a petrophysical nature of a carbonate reservoir system that is quite heterogeneous (Mazzullo, 2004).

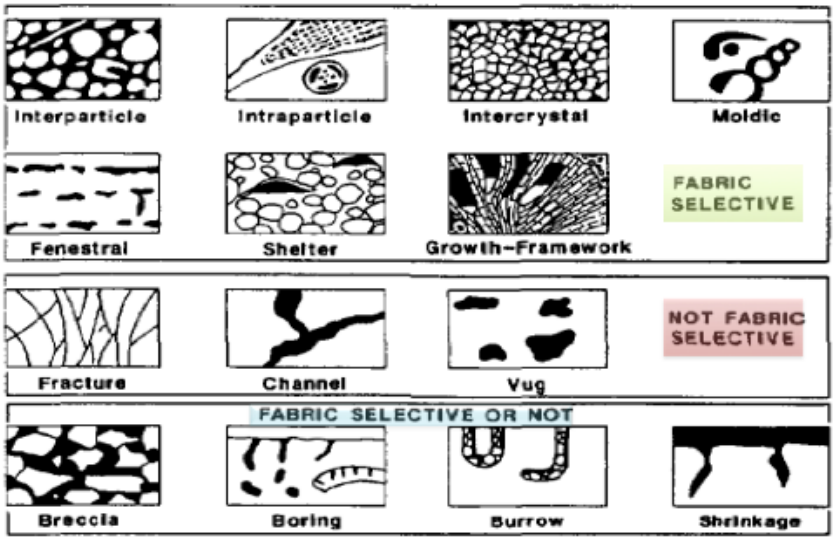

Figure 1-0Diagram of the three major porosity groups exhibited in carbonate rocks (Longman, 1981).

1.2 Dolomitization

Dolomitization is a diagenetic process that occurs when Mg^{2+} ions replace the Ca^{2+} ions in calcite, converting limestone into dolostone (Machel, 2004). Dolomite has a smaller molar volume than calcite; therefore, mole-mole replacement during dolomitization will give way for an increase in rock pore volume (Warren, 2000). Although the origin of dolomitization is still up for debate, the two following models are the most commonly associated with the process of dolomitization (Figure 1-3). If the limestone initially deposits in a shallow marine environment, then dolomitization can take place when fresh meteoric water mixes with marine seawater (Welch, 2001). This model is known as the hyposaline mixing-zone "Dorag" model (Welch, 2001). If the limestone deposits in an intertidal to supratidal evaporitic environment, periods of highstand flooding can pump in hypersaline Mg^{2+}- rich brine, which then causes partial evaporitic mineral replacement, otherwise known as the seepage-reflux dolomitization model (Welch, 2001). The origin of dolostone can occur from either scenario of burial diagenesis, as long as there's at least 5-30% pore volumes of seawater interacting with the calcite (Badiozamani, 1973; Warren, 2000). Depending on the window and type of deposition, whether it is marine or continental, the exposed carbonate platform may undergo just one or both burial diagenetic settings of dolomitization (Figure 3) (Machel, 2004).

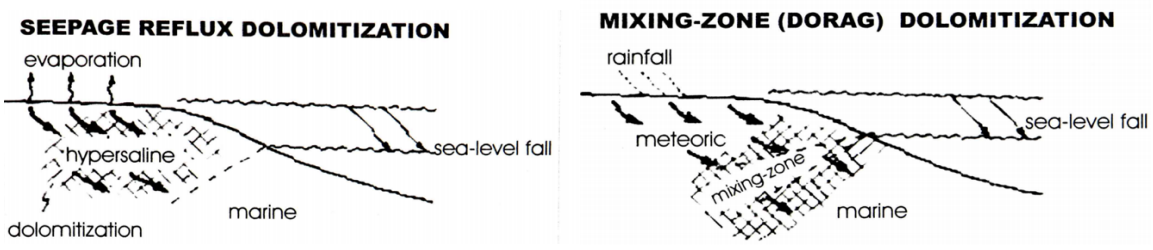

Figure 1-3. Seepage-reflux model and mixing-zone "Dorag" model for dolomitization (Welch, 2001).

1.3 Significance

Understanding the interactions that occur at the onset of deposition as well as throughout the post-depositional process can serve as a vital tool in determining whether or not a rock formation is deemed fit to be a viable reservoir rock (Syed et al., 2010). Once a carbonate rock is deposited, it can preserve its original granular (or skeletal) framework in order to maintain its original porosity, otherwise known as primary porosity (Syed et al., 2010). However, the original porosity can change during the process of diagenesis, due to the chemical interactions that occur when subjected to further burial and compaction (Syed et al., 2010). This creates secondary porosity which, depending on the lithologic alterations that take place during the subsequent stages of diagenesis, will either create more porosity or inhibit the preexisting void space (Syed et al., 2010).

The Viola Limestone Formation is a carbonate reservoir that is widely exposed throughout Texas, Oklahoma, Nebraska, Missouri and Kansas, yielding moderate production rates of oil and gas throughout its course (Carlson and Newell, 1997). Specifically, in south-central Kansas, as of 2013, the Viola Limestone "Pool" in the Herd, Bird East and Box Ranch oil fields in Comanche County, located just east of Clark County (Figure 1-4), collectively produced as much as 2.2 million barrels of oil (BO) and 9.7 billion cubic feet of gas (BCFG) (Richardson, 2013). In Kansas, the Viola Ls. has produced significantly more than it has in other states, with exception of Oklahoma (Carlson and Newell, 1997). Although the production rate of the Viola in oil fields in south-central Kansas is partly contingent on the geologic structure and overall petroleum system, much of the Viola limestone's reservoir quality can be attributed to the aggregate effect of the rock's depositional environment and diagenetic alterations (Richardson, 2013; Syed et al., 2010).

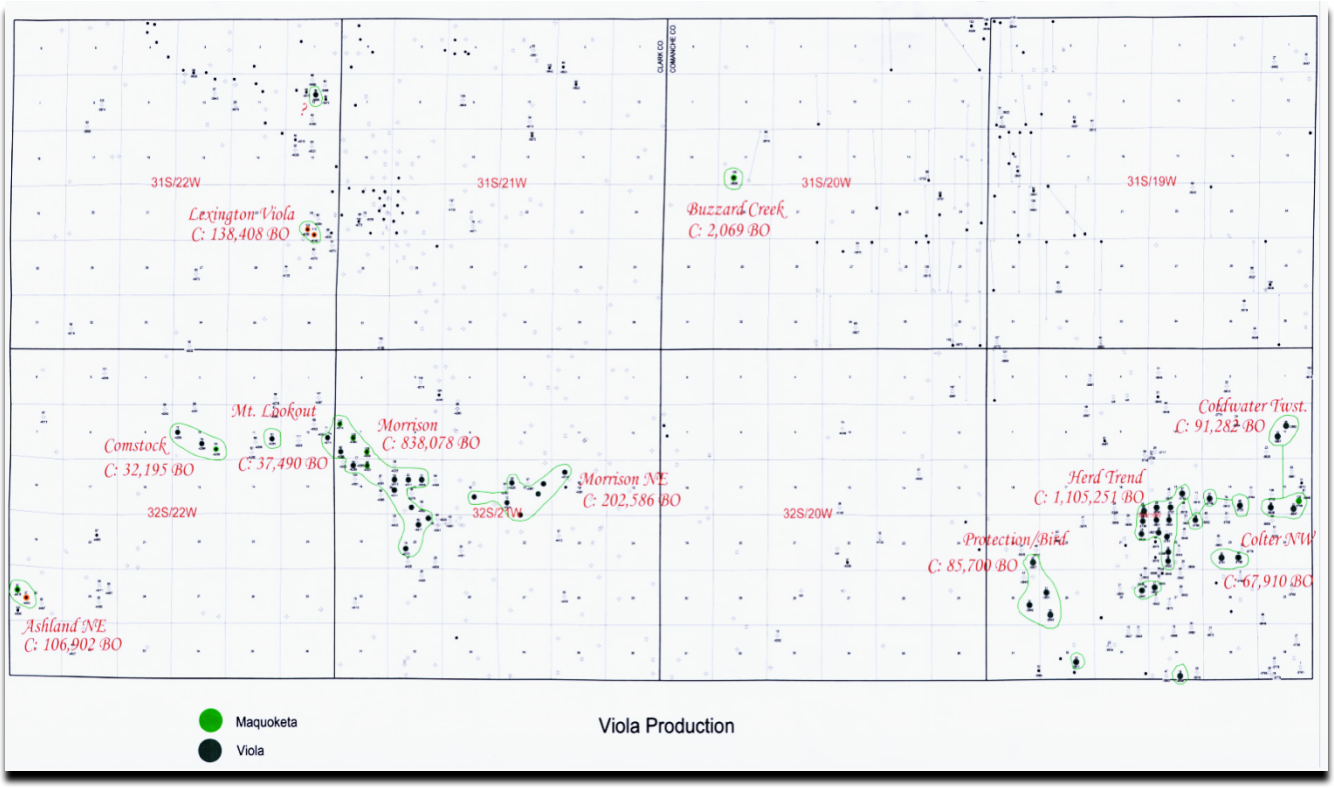

Figure 1-4. Map of current oil and gas fields of both Clark County and Comanche County, south-central Kansas (Richardson, 2013).

1.4 Geologic Setting

The Viola Limestone was deposited during the Middle Ordovician in a tidal environment, possibly during the high stand of an epeiric inland sea (Figure 1-5) (Bornemann et al., 1982). This epeiric inland sea covered most of the North American interior, depositing the Viola extensively across the mid-continent region (Figure 1-6) (Bornemann et al., 1982; Sloss, 1987). At the time of the Ordovician period, the mid-continent was a relativity flat low-lying area, therefore making it susceptible to flooding from epicontinental seaways (Harries, 2009). According to sequence stratigraphy, the high stand of this epeiric inland sea transgressed across present-day Kansas, depositing a basal limestone along the paleo shoreline (Bornemann et al., 1982). Episodic periods of epeiric inland seas persisted throughout the Paleozoic and Mesozoic

eras, with the Viola limestone as one of these prime examples of sediment depositing during a time of high eustatic sea levels sweeping across the continental mainland (Bornemann et al., 1982; Harries, 2009).

Figure 1-5. Illustration portraying epeiric inland sea covering all of Kansas during the Middle-Ordovician period (Blakey, 2016).

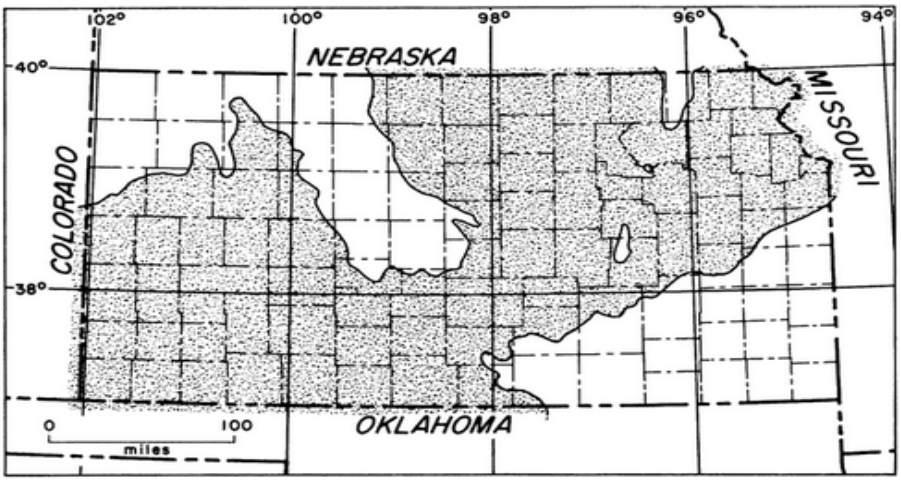

Figure 1-6. Geologic map exhibiting the lateral extension of the Viola limestone across the mid-continent region (Merriam, 1963).

Although the Viola limestone of the Morrison Northeast Field was initially deposited in an unperturbed flat environment, the adjacent geologic provinces were subjected to the succeeding periods of faulting and uplift, prompting the already buried Viola limestone to be exposed to the surrounding stress in south-central Kansas (Merriam, 1963). In particular, at the time of the Ordovician, the Pratt Anticline in southeastern Kansas was already overlain by deposited Viola sediment (Figure 1-7), indicating that the geologic region of the present-day Pratt Anticline was at one point a submarine environment (Bornemann et al., 1982). It has also been observed that outcrops of the Viola limestone are absent in Kansas, further signifying that the Viola limestone deposited prior to substantial uplift events (Bornemann et al., 1982; Merriam, 1963). Aside from the fact that the Middle Ordovician-aged Viola limestone is not exposed at the surface in Kansas, it is also important to note that the deeply buried Viola in south-central Kansas has undergone periods of erosion, resulting in an unconformity with the overlying Late Ordovician-aged Maquoketa Shale/Early Mississippian-aged Kinderhook Shale (Figure 1-8) (Bornemann et al., 1982; Richardson, 2013). Since a shale formation uncomformibly overlays the Middle Ordovician-aged Viola Formation, it is possible for a stratigraphic trap to have formed in response to the non-porous overlying shale abruptly sealing off hydrocarbons at the top of the porous Viola limestone facies (Richardson, 2013).

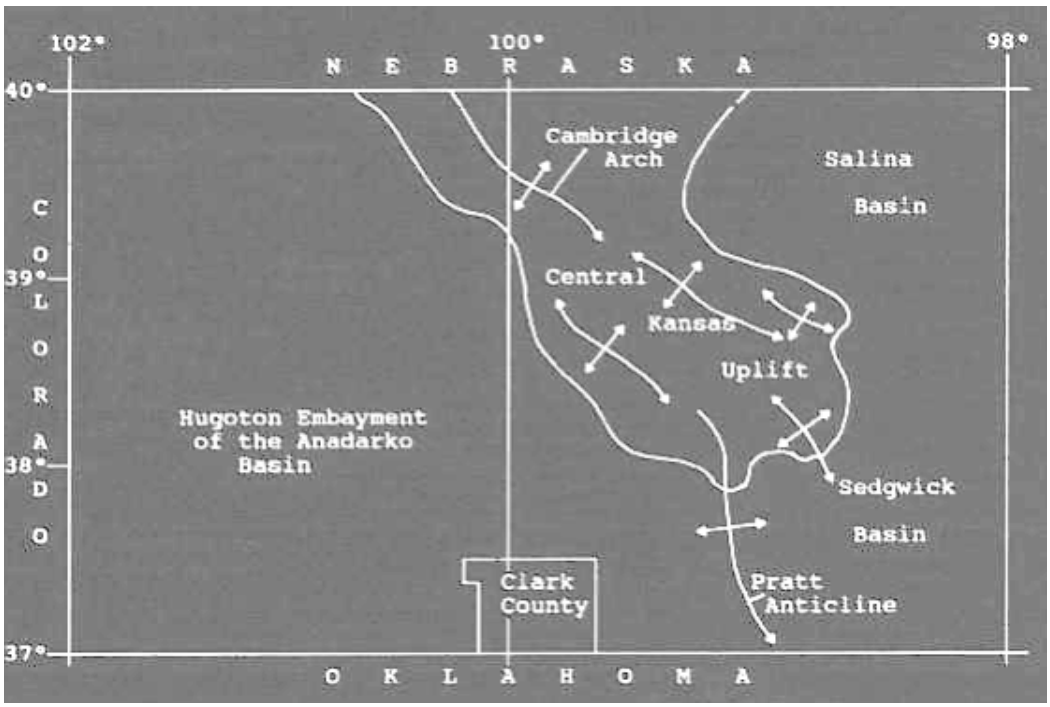

Figure 1-7. Map exhibiting the prominent structural features of Kansas during the Paleozoic era (Green and Fairer, 1995).

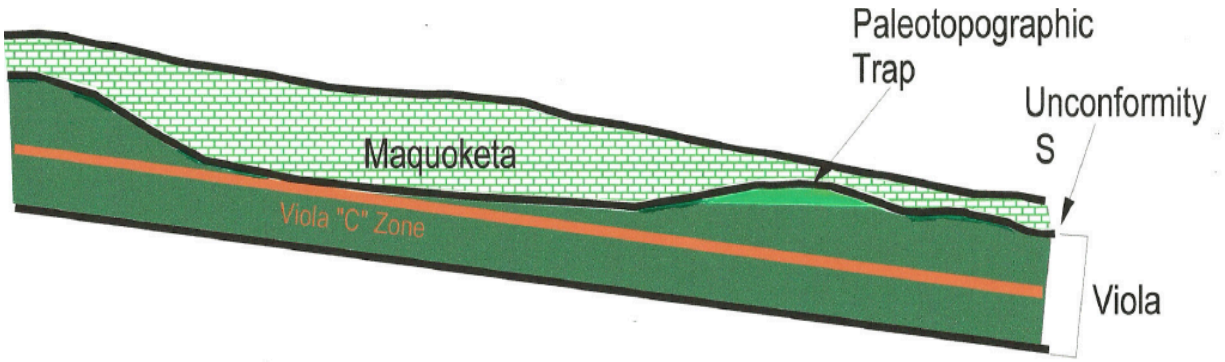

Figure 1-8. Illustration of the unconformity present between the Viola Ls. and Mississippian Maquoketa Sh. A paleotopographic trap formed as a result of the overlying Maquoketa Sh. sealing the upper facies of the Viola Ls. (Richardson, 2003).

1.5 Study Area

The study area for this research is the Middle Ordovician-aged (470-440 Mya) Viola limestone formation found in the Morrison Northeast Field of Clark County, south-central Kansas. Drill-cutting samples of the Viola limestone were collected from the Stephen's Ranch within the Morrison Northeast Field. The Morrison Northeast Field straddles the Hugoton Embayment of the Anadarko Basin to the southwest and the Central Kansas Uplift and Pratt Anticline to the east (Figure 1-9) (Green and Fairer, 1995). The Morrison Northeast Field of Clark County is centrally located in a structurally and stratigraphically complex area, due to the surrounding stresses from subsequent uplift, faulting and erosional events that occurred at the time of the Late Mississippian (~326 Mya) and continued throughout the rest of the Middle to Late Paleozoic era (Merriam, 1963).

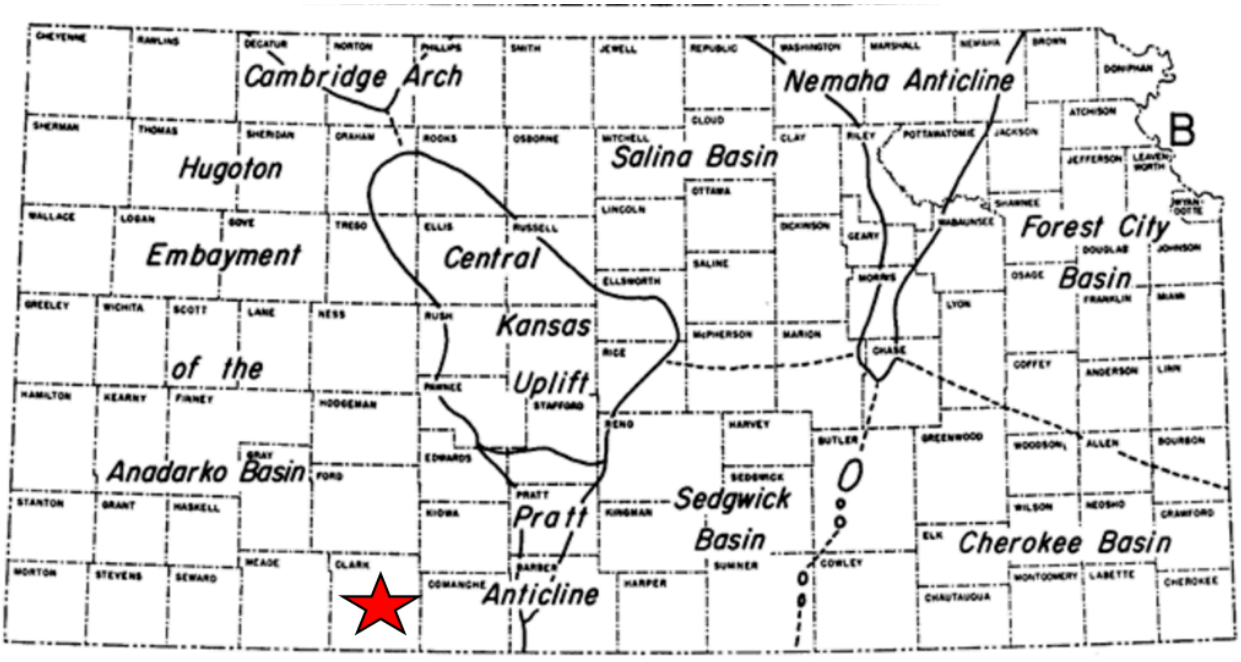

Figure 1-9. Map of Kansas uplifts and basins (Merriam, 1963).

1.6 Previous and Concurrent Research

Hydrocarbon production is typically dependent on the structure of the target formation. However, in the case of the Viola limestone in the Morrison Northeast field, the structural position seems to have little consequence for the field's production. Previous structure maps of the Viola Ls. formation in Comanche County, south-central Kansas, in conjunction with the seismic facies interpretation of the Viola subsurface at Stephen's Ranch suggest that subsurface structure may not be the primary control on the economic production of the Viola limestone in south-central Kansas (Richardson, 2013). Therefore, other factors that would internally affect the Viola limestone's petrophysical properties must be considered, such as the facies' depositional environment or diagenetic alterations (Richardson, 2013). Although the post-depositional effects of diagenesis can influence the sedimentary rock's textural fabric and mineralogical composition, the rock's depositional environment must also be accounted for. Along with diagenetic alterations, these intrinsic rock properties derived from the constituent allochem assemblage at the time of deposition may provide further insight into the Viola limestone's fluid flow properties (Syed et al., 2010).

1.7 Hypothesis

In order to improve our understanding of the overall reservoir quality of the Viola limestone, it must first be established which facies in particular is/are controlling the production of oil and gas within this carbonate reservoir. Secondly, it must be determined whether the porosity and permeability are strictly governed by the depositional environment, entirely influenced by diagenesis, or influenced by the convergence of both processes (Syed et al., 2010). This petrographic study was completed as a complement to the seismic attribute analysis of the Viola limestone that was previously completed by fellow geophysics graduate student, Andrew Vohs

(Vohs, 2016) and advisor, Dr. Abdelmoneam Raef, with the anticipation of potentially providing a proper workflow on correlating the zones that yield higher productivity from both a geological and geophysical standpoint.

The Morrison Northeast field's highest production rates occur irregularly across the field, with no obvious correlation to the location of structural highs, which can be seen on the following Viola time structure map of the Morrison Northeast field (Figure 1-10) (Raef et al., 2016). This time structure map was specifically generated to look at the top of the Viola Ls. to the top of the Viola's "C" Zone facies (Richardson, 2013; St. Clair, 1985). Based on previous research done by (Richardson, 2013), there was a particular interest from the top of the Viola to the top of the "C" Zone facies in the Herd field, approximately 12 miles east of this study. According to Richardson, the primary hydrocarbon production is coming from where there are "paleotopographic highs" above the "C" Zone facies where the productive "A" and "B" zones are preserved (Figure 1-11).

With an apparent lack of structural trapping in the field, the question remains as to what factors are controlling this oil and gas production. For this study, both the lithofacies and seismic facies of the Viola limestone were further correlated, in order to establish how and why only a few wells in the Stephens Ranch lease are currently producing, while the remainder have never produced or have recently been abandoned.

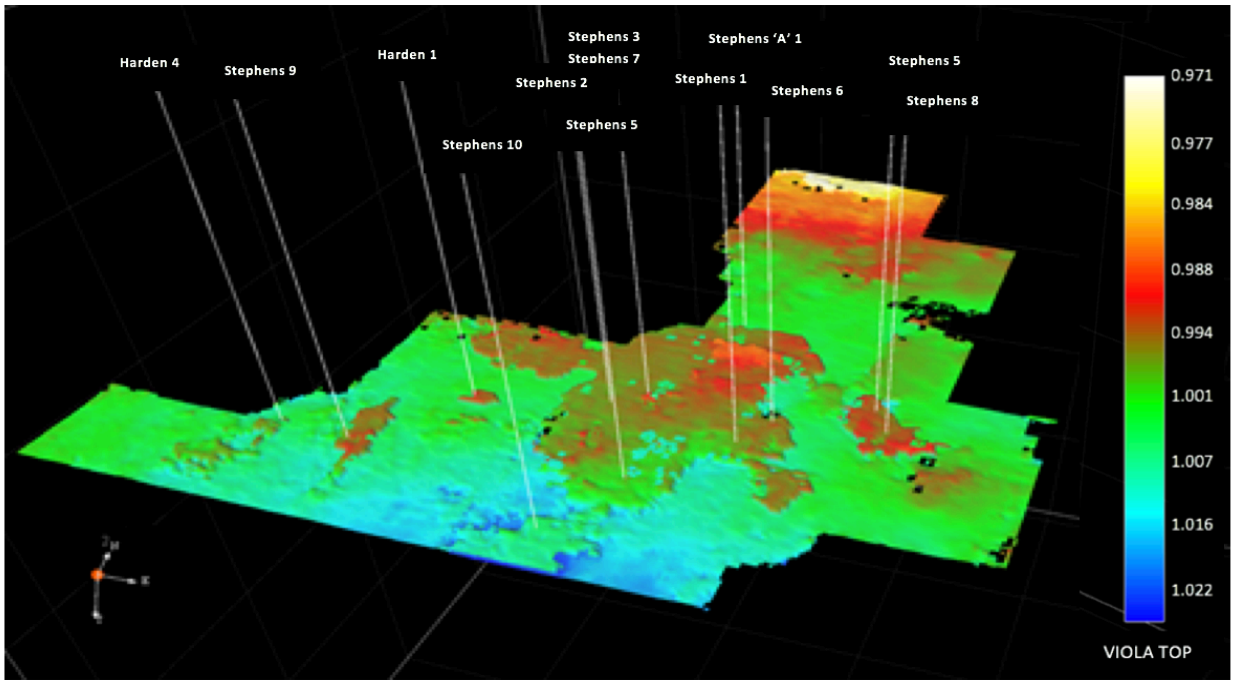

Figure 1-10. Time structure map from the top of the Viola Ls. to the Viola "C" zone, which occurs about 8ms (generally 20-40ft deep) (Raef et al., 2016).

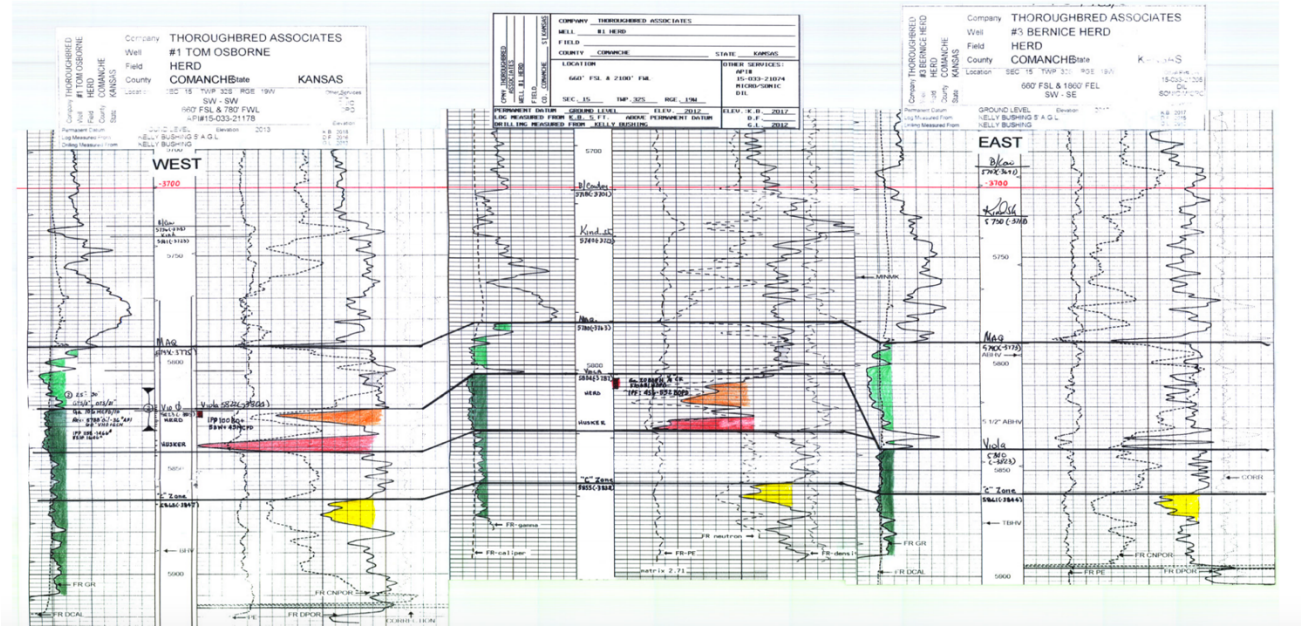

Figure 1-11. Detailed cross-section of the top of the Viola Ls. (in orange) correlated across producing wells in the Herd field of Comanche County. The "A" zone (orange) and "B" zone (red) are the productive intervals. The "C" Zone is also correlated (in yellow) 20ft-40ft below the top of the Viola Ls. (Richardson, 2013).

Chapter 2 - Background

2.1 Stratigraphy

There are four major facies represented within the Viola limestone of south-central Kansas (Figure 2-1) (Bornemann et al., 1982). The facies of the Viola limestone that have been consistently observed in south-central Kansas (Figure 2-2) include the “D” Zone basal fossiliferous limestone, the “C” Zone cherty dolomitic limestone, “B” Zone upper fossiliferous limestone and the “A” Zone upper cherty dolomitic limestone (Bornemann et al., 1982). This facies sequence is indicative of a large marine transgression event that occurred during the Middle to Late Ordovician and deposited a series of carbonate rocks across the Mid-Continent (Bornemann et al., 1982). The facies alternate between sparry limestone and dolomitic limestone, suggesting a pattern of cyclicity present in the Viola limestone (Bornemann et al., 1982). The following facies units provide the general description of Viola limestone cores that were observed in Barber and Pratt County, just east of Clark County (Bornemann et al., 1982).

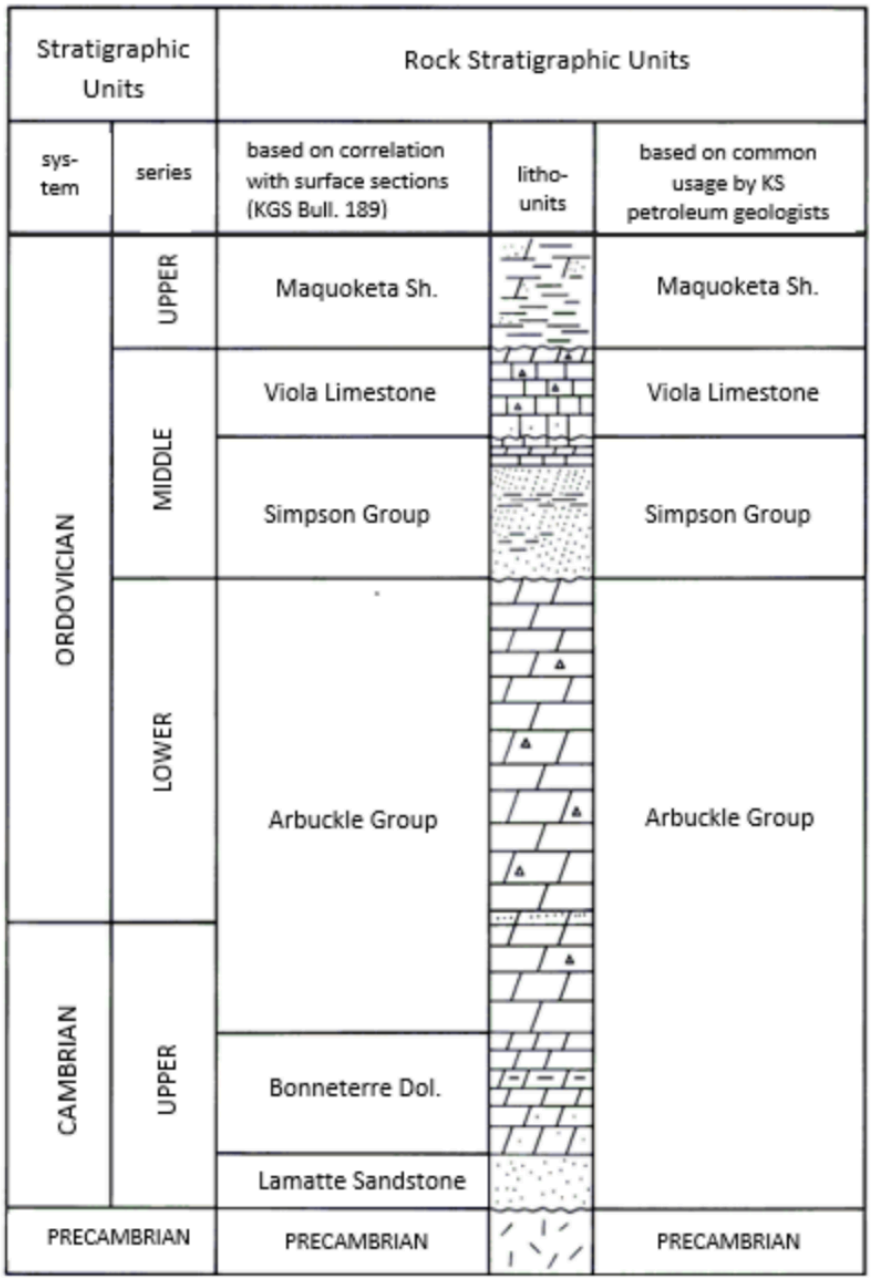

Figure 2-1.Stratigraphic column with formations in study area. Note Viola limestone and overlying Maquoketa shale (Cole, 1975).

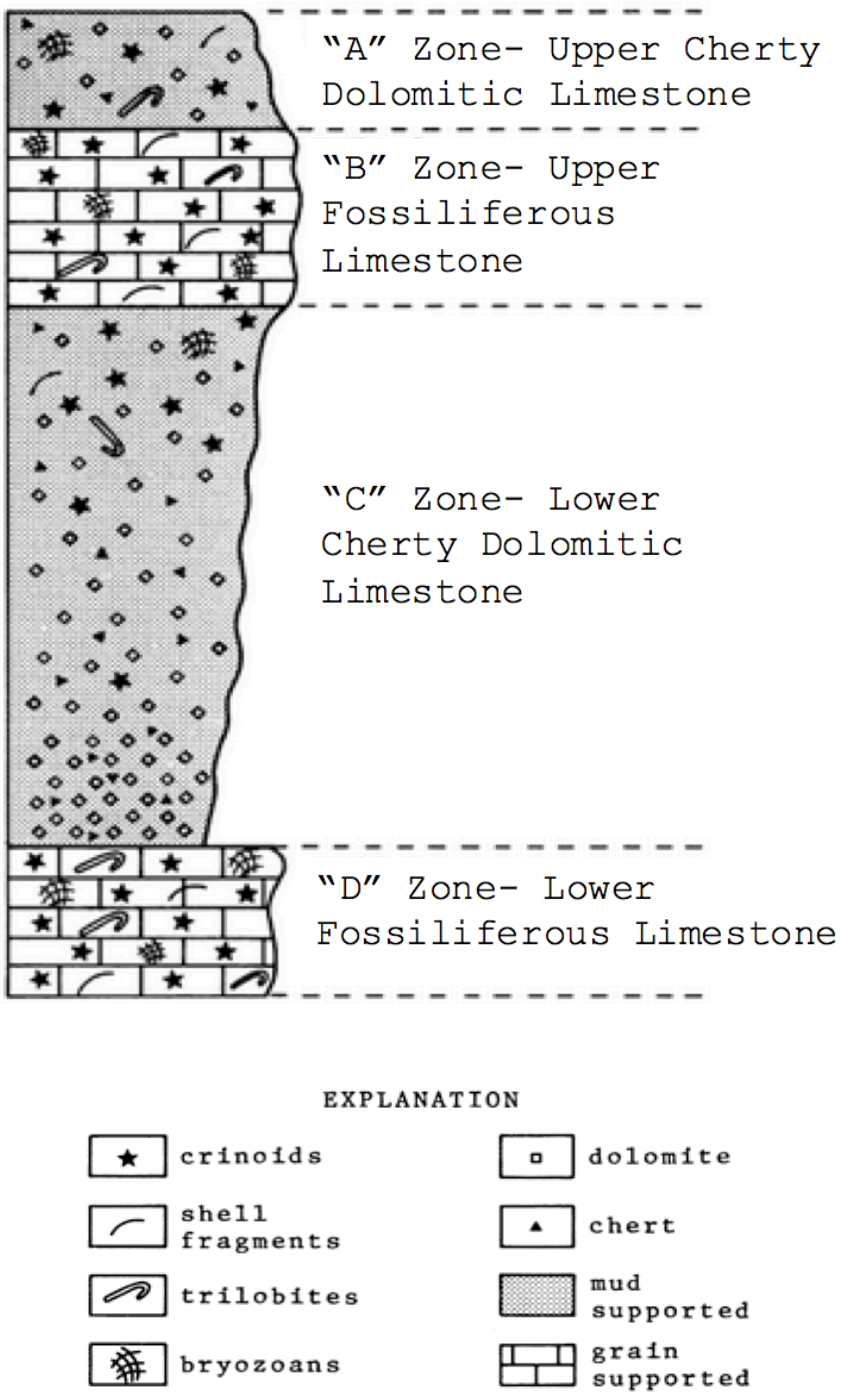

Figure 2-2. This diagram shows the four facies that exhibit a cyclic pattern within the stratigraphic section of the Viola Limestone in south-central Kansas from (St. Clair, 1985).

2.1.1 “D” Zone: Basal Fossiliferous Limestone

The basal facies is a fossiliferous limestone, specifically consisting of grainstones and packstones with the presence of crinoids, trilobites and bryozoans, along with minor mollusks and brachiopods (Bornemann et al., 1982). This basal limestone can range anywhere from 5 to 25 feet in thickness in south-central Kansas (Bornemann et al., 1982). This limestone facies is indicative of marine transgression, and was possibly deposited in a marine setting of higher-energy conditions (Bornemann et al., 1982). The textural fabric typically seen in the basal limestone is a moldic fabric, in which the structure is intact but many of the fossil shells have been dissolved out (Bornemann et al., 1982)

2.1.2 “C” Zone: Cherty Dolomitic Limestone

The cherty dolomitic limestone facies that overlays the basal limestone is typically micritic, and composed predominantly of dolomite and chert, along with minor fossiliferous wackestones (Bornemann et al., 1982). The presence of dolomite, rather than calcite or aragonite, suggests that dolomitization either occurred as the sea retreated and the sediment was sub-aerially exposed, or at the onset of diagenesis in a shallow, low-energy, high-saline environment (Bornemann et al., 1982). The prominent texture observed in the dolomitic limestone is a fabric-supported intercrystalline porosity, which can suggest that both primary or secondary porosity is present between the equant crystals within the dolomitic cement (Bornemann et al., 1982). It has also been observed that this facies can be as much as 100ft thick in the Viola limestone, yet it is absent in some areas, indicating that after the second facies was deposited, there may have been an erosional event that ensued (Bornemann et al., 1982).

2.1.3 “B” Zone: Fossiliferous Limestone

Similar to the basal fossiliferous limestone, the third facies of the Viola limestone is composed of the wacke/packstones with ooids, trilobites, crinoids and bryozoans, and other minor organisms (Bornemann et al., 1982). This facies is relatively thin in southern Kansas, and is only prominent in western Kansas, possibly indicating another erosional event having transpired, or a possible change in sediment distribution at the time of deposition (Bornemann et al., 1982).

2.1.4 “A” Zone: Upper Cherty Dolomitic Limestone

The upper cherty dolomitic limestone is very similar to Unit C (Bornemann et al., 1982). With the alternating fashion of grain-supported fossiliferous limestone to a mud-supported dolomitic limestone, it is evident that the epeiric inland sea levels fluctuated during this period, as there is a prominent cyclic pattern exhibited in the facies of the Viola limestone (Bornemann et al., 1982).

2.2 Morrison Northeast Field

The general study area for this research is the Morrison Northeast Field of Clark County, Kansas. The wells included in this study are located in Stephen’s Ranch, which is a land property in the Morrison Northeast Field with oil and gas wells that are mainly operated by Coral Coast Petroleum, LLC. The Stephen’s Ranch property comprises the northeast corner and most of the southern portion of the oil field (Figure 2-3). Drill-cuttings were obtained from each of the wells, in order to find a correlation between the Viola’s lithologic features and petrophysical properties. Assessing each of the drill cuttings’ lithologic and textural features make it possible to determine which rock properties are controlling past and current oil and gas production in Stephen’s Ranch. The current well status for many of the Stephens Ranch wells is “D&A” which denotes a

plugged and abandoned well, highlighted in red in (Table 2-1). Even so, there are a few remaining wells, such as Stephens 1, Stephens 2, Stephens 4, Stephens 6 and Stephens 7, which are all still currently producing oil and gas "O&G" (highlighted in green) from the Viola Ls. formation, roughly targeting production around 6400 to 6500 feet MD (measured depth) (KGS, 2016).

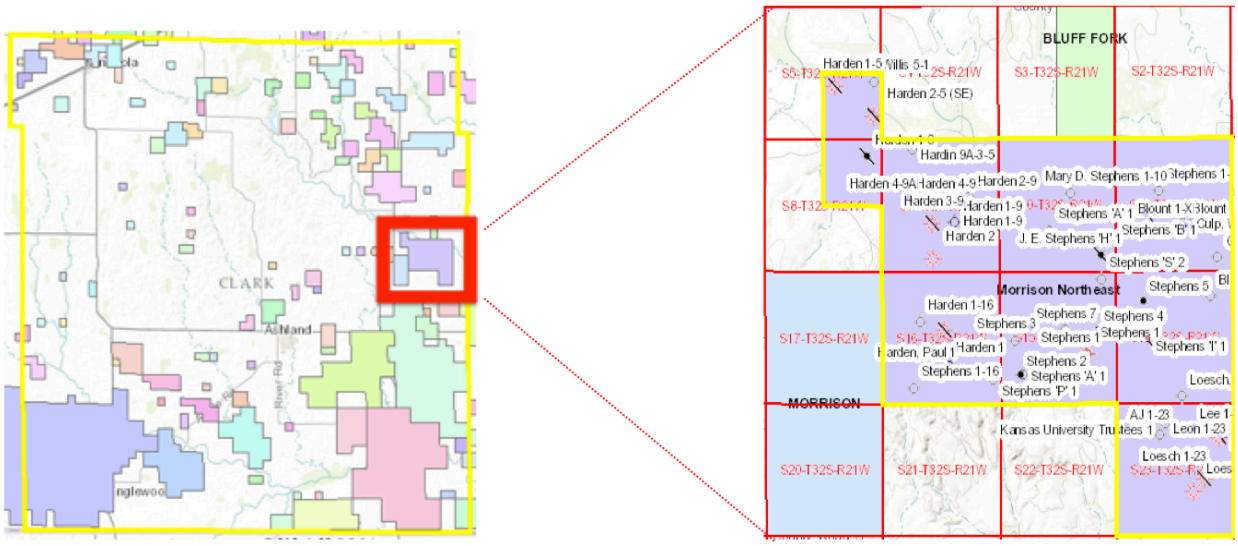

Figure 2-3. Base map from KGS of wells in the Morrison Northeast Field (KGS, 2016).

Well	API	Field	Current Status	Completion Date	Year	Oil Production (bbls)	Gas Production (mcf)
Stephens 1	15-025-10027	Morrison NE	GAS	4/22/2011	2011 2012 2013 2014 2015	44,694 8,066 2,081 799 478*	34,163 113,997 109,555 83,198 25,240**
Stephens 2	15-025-21527	Morrison NE	O&G	9/19/2011	2011 2012 2013 2014 2015	2,371 42,803 19,395 6,312 1,248	N/A
Stephens 3	15-025-21532	Morrison NE	D&A	10/27/2011	2011	D&A	D&A
Stephens 4	15-025-21539	Morrison NE	O&G	4/27/2012	2012 2013 2014 2015	46,430 18,113 11,151 2,286**	N/A
Stephens 5	15-025-21543	Morrison NE	O&G to SWD	6/22/2012	2012 2013	3,992 494	2648 0
Stephens 6	15-025-21547	Wildcat	O&G	12/3/2012	2013 3014 2015	6,701 1,608 306*	10,938 4,560 1,709**
Stephens 7	15-025-21554	Morrison NE	O&G	2/14/2013	2013 3014 2015	15,293 636 140***	21,465 0 240**
Stephens 8	15-025-21558	Morrison NE	D&A	3/16/2013	2013	D&A	D&A
Stephens 9	15-025-21561	Wildcat	O&G	6/12/2013	2013 3014 2015 2016	0 124 0 0	3,373 155,408 90,217 19,162
Stephens 10	150925-21563	Morrison NE	D&A	9/23/2013	2013	N/A	N/A
Harden 1	15-025-21545	Morrison	O&G	10/12/2012	2012 2013 2014 2015*	4,384 13,191 1,265 166	5,014 48,049 639***** 0

*Through 5-2015, **Through 7-2015, ***Combined gas production of Stephens 1,2&4, ****Through 2-2015, *****Through 8-2014, ******Through 5-2014.

Table 2-1. Chart showing the current oil and gas production of wells of interest. Wells marked in green are wells still producing O&G or GAS. Wells marked in red are denoted as plugged D&A (Provided by KGS database, 2016).

Chapter 3 - Methods

Reservoir studies typically rely upon examination of core. None of the wells in the Stephens Ranch were cored, which constrained the methods available to characterize the reservoir in this field. A well log analysis was conducted to establish which wells to incorporate into this study. This was combined with production history of each well to select the most productive wells, together with wells that were the least productive throughout the field's history. The variation in productivity is presumably controlled by reservoir properties. The petrographic data collected in this study should explain any disparities in production rates across the Stephens Ranch lease area.

3.1 Well Log Analysis

Stratigraphic correlations of the Viola limestone formation were made across the Morrison Northeast Field by analyzing each of the well logs available (Figure 3-1). Recognizing the Gamma Ray, Spontaneous Potential, Resistivity, Density and Neutron well log signatures of the Viola Limestone in each of the Stephens Ranch wells sections, provided an easily identifiable Viola facies interpretation that helped determine which wells to include in this study. The Viola section was compared between productive and non-productive wells to understand where the productive facies (if present) occurred in each well, and what the log signature was for this facies. All of the data were recorded into the computer database for the project.

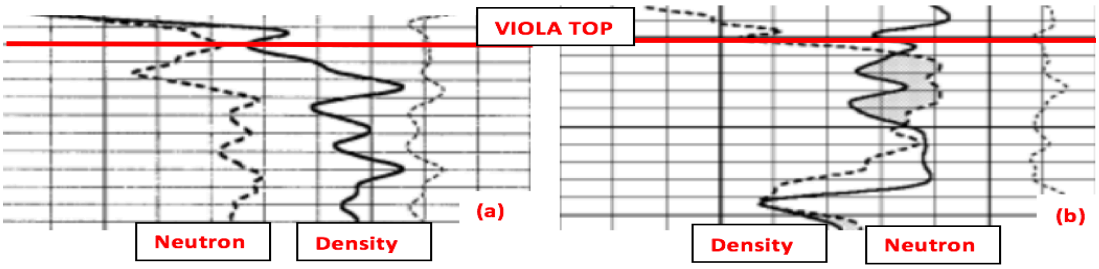

Figure 3-1. Example of correlating Viola Ls. "top" across wells using Density and Neutron logs. Porosity logs on Stephens 3 well on left (15.a) and Harden 1 well on right (15.b).

3.15 Sample Selection

Based upon the previously described well log analyses, and the availability of well cuttings, five wells were selected for petrographic examination. The cuttings from the Stephens 4, 6, 9, 8 and 3 wells were obtained from the KGS Sample library in Wichita, Kansas. The specific drill-cuttings were collected from each desired sampling depth based upon geologic reports available from the KGS website, and the well logs for each specific well. The cuttings were further separated by a detailed lithologic examination of the rock material's color, size, shape and porosity using a binocular microscope as described in the next section.

The cuttings for each of the wells were hand-picked from the interval packets containing drill-cuttings correlating to the rotary lag time that matched the last few feet of the overlying Maquoketa shale and the top of the underlying Viola limestone lithofacies. The individual lithofacies of the Viola limestone were quite recognizable and easy to pick out. When picking through each of the well's cuttings, it was evident as to which cuttings were the thin, overlying Maquoketa shale, in comparison to the cuttings that represented the Viola limestone.

3.2 Thin Section Preparation

Thin sections were prepared from each of the sets of drill cuttings separated. Cuttings diagnostic for each of the wells were collected and picked in order to record details of the borehole lithology, as well as examined for additional petrographic analysis (Figure 3-2). After the drill-cuttings were examined with a binocular microscope, the cuttings were then mounted to a glass slide. During the mounting process, the cuttings were impregnated with blue epoxy and then placed within a vacuum chamber for 1 minute to ensure that all of the air was extracted within and between grains, such that the dyed epoxy filled all of the void spaces. The blue epoxy was used to make it easier to examine the shapes and sizes of pores and, hence, to better

understand the natures of the porosity in each rock. After the cuttings were mounted to the glass slides, they were manually inserted on the Hilquist grinding machine. Each thin section slide was carefully ground for approximately 30 seconds while gradually decreasing the distance to the grinding wheel until the desired thickness of 30 microns was achieved. After grinding all of the slides, the slides were polished to remove the abrasive saw markings. The thin sections were then successively placed on a polishing wheel with 2000/2500 fine grade sandpaper, and polished on the wheel by hand (Figure 3-3). Light pressure was applied to the thin sections as they were moved in a circular motion on the wheel for about 45 seconds, or until all of the rough saw marks and scratches were removed. Once all of the thin sections were polished, they were ready for petrographic inspection.

3.25 Petrographic Analysis

A petrographic microscope was used to determine the optical mineralogy as well as the structural fabric and type of porosity, which could then infer depositional environment and/or stage of diagenesis within each of the samples. Petrographic examination of the well cuttings was utilized to corroborate which factors inhibit or promote hydrocarbon production.

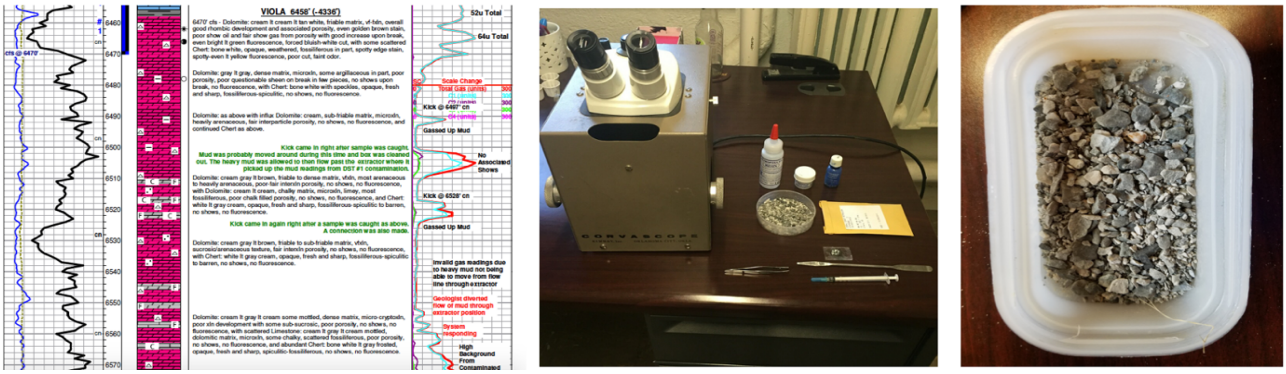

Figure 3-2. Example workflow of correlating drill cuttings to drill-time in geologic reports.

Figure 3-3. Photographs of polishing mounted thin sections on grinding saw.

3.3 Optical Software Application

Photomicrographs of the thin sections at 10X magnification in plane-polarized were uploaded to a Photoshop-based software, Adobe Photoshop, in order to assign a blue color palette to each image. This blue color palette was examined using the optical software, ImageJ jPOR, as a rapid and precise way of estimating total porosity. With the applied blue color palette, ImageJ jPOR can quickly isolate the blue epoxy from the rock matrix, and estimate the percentage of blue epoxy that is present in the image (Figure 3-4). The percentage of blue epoxy in each image represents the total void space present in each of the thin sections, which is a measure of total porosity present in each thin section.

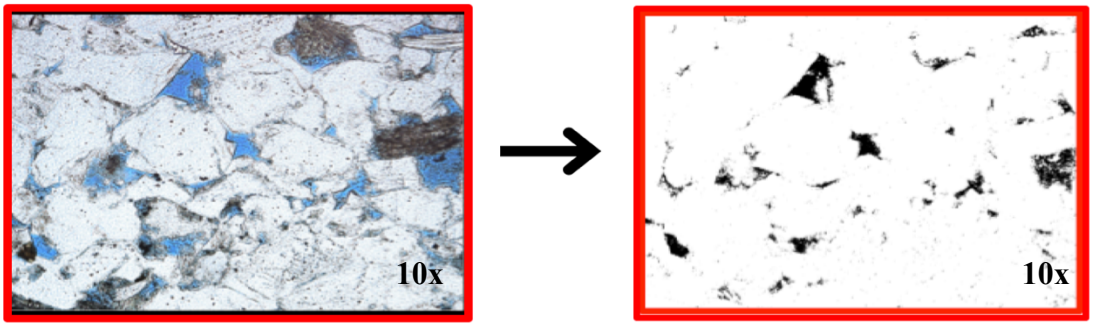

Figure 3-4. Example of optical PPL thin section image of the Tonkawa Sandstone on the left, and corresponding picture with isolated blue color palette applied on the right.

3.4 SEM and EDS Imaging

The polished thin sections were taken to the University of Kansas' Microscopy and Analytical Imaging Laboratory to examine under SEM with EDS (scanning electron microscope with energy dispersive X-ray spectroscopy) detection on the FEI Versa 3D DualBeam. Due to the costly nature of the FEI Versa 3D DualBeam, only representative thin sections were imaged in order to obtain a diagnostic depiction of the different texture and porosity types exhibited across each of the Stephens Ranch wells.

The DualBeam EDS detector was used because it is more receptive than other tools at quantifying lighter elements in smaller abundances, and in the case for the DualBeam EDS, it can quantify all elements greater than fluorine (H. Shinogle, personal interview, 2016). Initial preparation for the DualBeam EDS detector required that all cover slips be removed from the thin section slides, as the absence of a cover slip aides in proper electron penetration of the samples. In order for the DualBeam to penetrate the thin section slide, a sputtering machine was utilized in order to coat all of the slides with conductive material. For the purpose of this study, platinum/palladium was used as the conductive material, as it allowed for higher electron bombardment on the sample, yielding higher-order quantitative results.

Once the thin sections slides were coated with the conductive platinum/palladium material, they were then individually loaded into the DualBeam sample chamber and evacuated to 5 mbar (H. Shinogle, personal interview, 2016). The DualBeam operates using the xT Microscope Server software was subsequently turned on in order to communicate with the DualBeam vacuum. Once the software was operational, the vacuum chamber was closed in order for the vent process to initiate. After the vent process was confirmed, the sample was placed on a highly precise stage, centered on the stage approximately 10mm below the beam, in order to establish a

fixed beam penetration. Once the slide was properly loaded into the chamber, the pump was then turned on. While the pump was running, an optical image of the sampled section would start to pixelate on the screen. The image produced needed to be modified by adjusting the beam focus and alignment to improve the image resolution. One of the major features of the xT Microscope Server software was that it can produce simultaneous images using both the standard ETD as well as the secondary ICE image detection, which aids in a proper image resolution comparison. Once the image detection was determined, the EDS detector was then initiated, producing a focused beam of electrons that bombarded the thin section sample. This was done in order to produce a series of X-Rays that emit characteristically high-energy particles from the sample, yielding diagnostic elemental peaks. These elemental peaks could then be viewed as quantitative elemental maps for each of the samples, when the Aztec software was implemented along with the EDS detector. Images of elemental maps can be found in Appendix A.

Overall, the SEM with EDS allows for detailed imaging at exceedingly high-orders of magnitude. These data provided much greater resolution of rock characteristics such as texture, porosity type, mineral composition, cement type, and facilitation a more detailed interpretation of diagenetic history. As will be shown below, this is critical to the evaluation and analysis of the role that porosity plays in the production of the Stephens Ranch wells (Cone and Kersey, 1992).

3.5 Petra Mapping Software

IHS Petra mapping software was used to construct a base map of the plotted oil and gas wells that were used in this study, along with other nearby wells in T32S-R21W (Figure 3-5). A structure map and cross-section of the Viola limestone was then generated in order to investigate the control of structure on production, and provide the well location and depth to the top of the Viola Ls. formation present in the Morrison Northeast field.

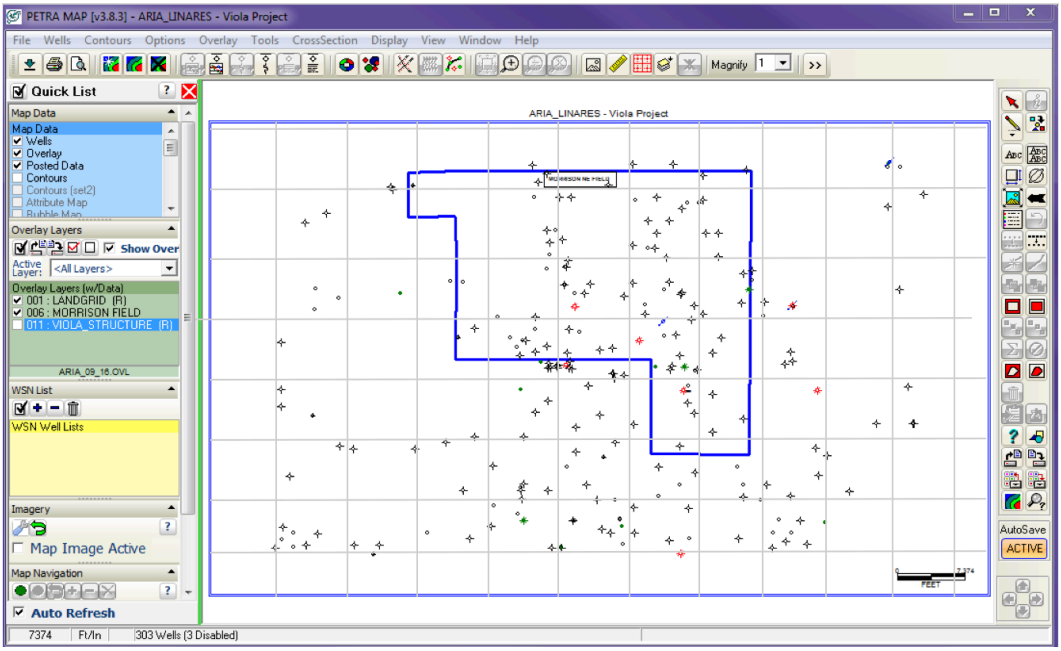

Figure 3-5. Base map of wells in the Morrison Northeast field (outlined in blue), as well as other nearby wells All wells were used to enhance well control when mapping the Viola Ls. structure across T32S-R21W.

Chapter 4 - Results

4.1 General Lithofacies Description

Examination of the drill cuttings is the most direct expression of the borehole lithology of the Stephens Ranch wells. The wells of interest, Stephens 1 through 10 and Harden 1, were each chosen based on their importance to Coral Coast LLC., as well as the availability of production and well log data for each of the wells. There are a total of four facies (Zones "A" to "D") in the Viola limestone, but in regards to this study, only the bottom of the overlying Maquoketa shale and the upper two facies of the Viola limestone, "A and B", were examined, based on the color, size and texture of the various cutting rock fragments.

The first set of cuttings examined were of the Maquoketa shale, in order to determine the depth each well transitioned into the underlying Viola limestone. The Maquoketa shale drill-cuttings exhibited a diagnostic tabular, gray shale with planar fracture. The Maquoketa was also easy to separate from the Viola in thin section, as it exhibited very fissile and tabular textural features, as well as more distinct argillaceous, with more clay content than the underlying Viola limestone.

The top "A" Zone Viola facies typically occurs as a thin 10 to 30-foot bed that lithologically includes bone white chert fragments, creamy cryptocrystalline limestone and sucrosic dolostone; this range of lithologies could easily be identified under the binocular microscope. In addition, the "A" Zone facies a minor presence of pyrite nodules occurring along the edges of the limestone, as well as a minor presence of fibrous anhydrite grains. When viewed under the microscope, it can be seen that the cryptocrystalline limestone consists of a very fine-grained particle dominated packstone/grainstone with sparse ooids and intraclast allochems surrounded by sparite cement. The dolostone in the "A" Zone facies has prominent euhedral

rhombic development, resulting in planar-equant intercrystalline porosity, fracture porosity, as well as some interooid and inter/intraparticle fabric-supporting porosity.

The “A” Zone grain-supported limestone and euhedral dolostone is stratigraphically followed by the “B” Zone facies, with the cuttings typically found at about 40 feet deep into the Viola limestone. In general, the “B” Zone facies exhibited a fossiliferous matrix-dominated wacke/packstone, as well as a notable decrease in both chert and dolostone content. The majority of the thin sections for this interval also predominantly consisted of limestone with a more micritic matrix that was partially dissolved. The “B” Zone facies appears to overall have sporadic vuggy and moldic porosity, as well as minor fracture porosity along the grain edges.

4.2 Stephens 4

Well cuttings were collected from where the Stephens 4 O&G well perforations target the Viola limestone at the (6330’- 6392’ c.90 min.) interval with respect to the geologic report and well log, and were then analyzed using a binocular microscope (Figure 4-1). Under the binocular microscope, dense microcrystalline limestone and sucrosic dolostone were both in high abundance. Thin sections from the same interval were then analyzed using a petrographic microscope. Collectively, the modal proportions of the producing interval mainly comprised of packstone/grainstone with some dolomite, and little chert present (Table 4-1). The Stephens 4 well target interval exhibits good fracture and fabric-supported porosity. The total optical porosity count (based on ImageJ jPOR) results for the petrographic image taken from the Stephens 4 (6390 c. 90 min.) was estimated at 20.5% (Figure 4-2). There is prominent fracture and intercrystalline porosity along individual rhombic dolostone grain edges (Figure 4-3). The EDS spectrum (Figure 4-4) shows a prominent Mg^{2+} peak, with an approximate Ca/Mg ratio of 3 (91:29) (Table 4-2).

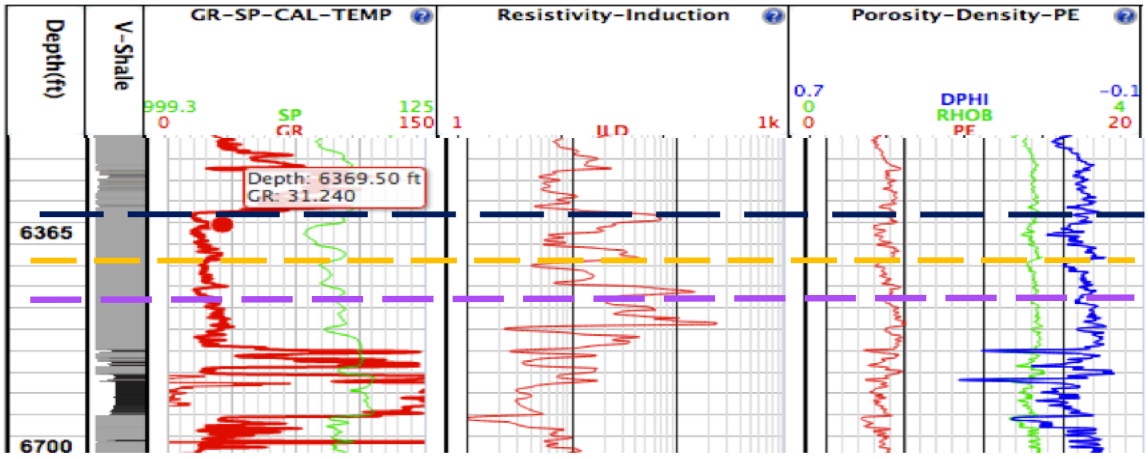

Figure 4-1. Viola Ls. top "A" Zone (in dark blue) "B" Zone top (in orange) "C" Zone top (in purple) for the Stephens 4 well.

Binocular Microscope Cuttings Description	Petrographic Microscope Thin Section Description	Total Estimated Porosity
Dense microcrystalline limestone cream grey dominant; fair sucrosic dolomite present; minor saturated stain; off white cream sharp/jagged chert present; fair porosity visible; no shows noted	Fossiliferous limestone packstone/grainstone dominant; some iron oxide staining on dolomite; Minor chert; not as nearly as much shale present; porosity visible along fractures in packstone; porosity seems to be along edges of grains; more fracture fabric-supported porosity present	20.5%

Table 4-1. Summary of cutting and thin section descriptions, as well as overall porosity percentage for the Stephens 4 well.

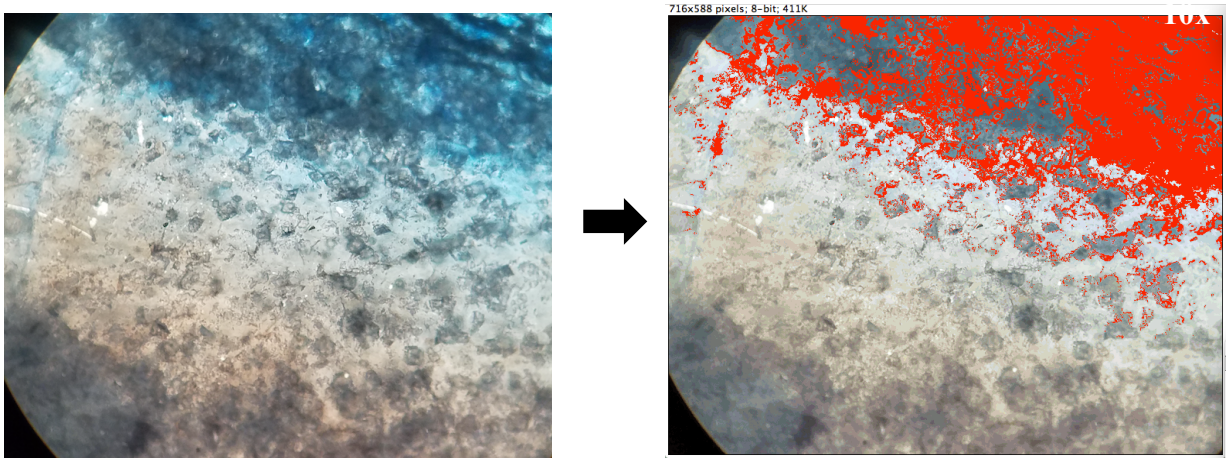

Figure 4-2. Optical PPL thin section image of the Viola Ls. in Stephens 4 well, and corresponding picture with isolated red color palette applied on the right to portray total porosity of 20.5%.

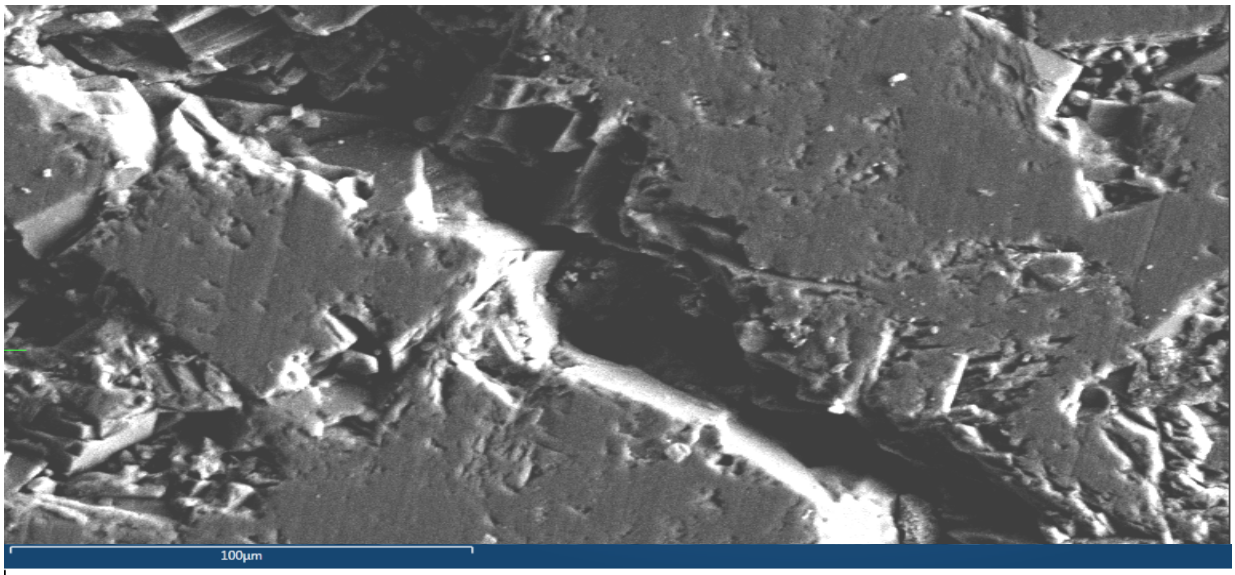

Figure 4-3. SEM DualBeam image at 100µm of Stephens 4 well, exhibiting fracture and intercrystalline porosity along dolostone grain edges.

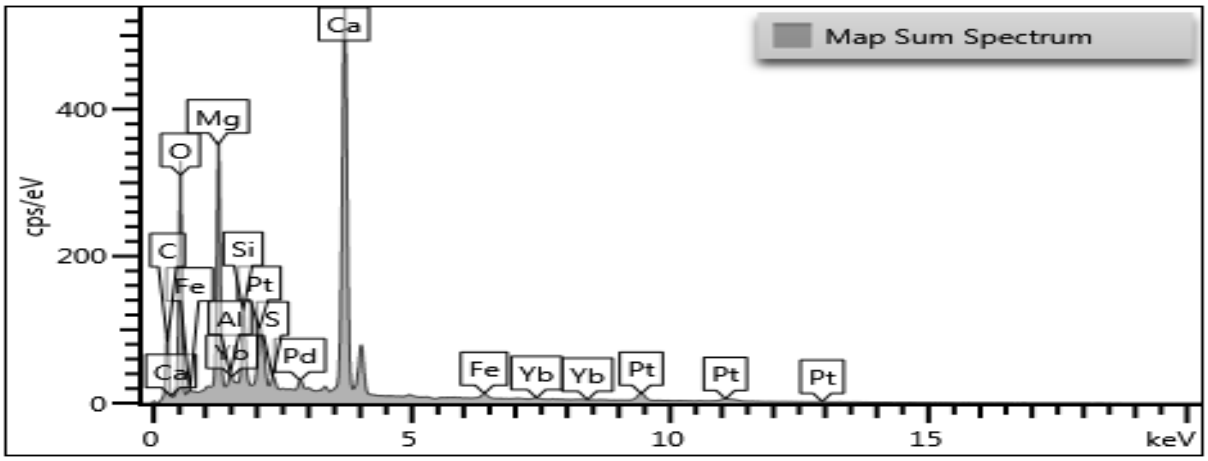

Figure 4-4. Graph of counts per section eV. Note spike in Ca/Mg depicted in map sum spectrum captured from Stephens 4 DualBeam image.

Element	Line Type	Apparent Concentration	k Ratio	Wt%	Wt% Sigma	Standard Label	Factory Standard
Ca	K series	91.36	0.81628	30.4	0.05	Wollastonite	Yes
Mg	K series	29.27	0.19409	13.4	0.03	MgO	Yes

Table 4-2. Summary of apparent concentrations and wt% of Ca/Mg, portraying spike in Mg^{2+} for Stephens 4 well.

4.3 Stephens 6

Well cuttings were collected from where the Stephens 6 O&G well perforations target the Viola limestone at the (6390'-6430') interval with respect to the geologic report and well log, and were then analyzed using a binocular microscope (Figure 4-5). Under the binocular microscope, dense cryptocrystalline limestone and sub-sucrosic dolostone with well-developed planar rhombs were visible. Thin sections from the same interval were then each analyzed using a petrographic microscope. Collectively, the producing interval mainly comprised of dolomite with equant crystal development, minor fossiliferous wacke/packstones, minor chert, and possible anhydrite replacement of calcite present (Table 4-3). The Stephens 6 well target interval exhibits good intercrystalline and interparticle porosity, as well as prevalent vuggy porosity. The total optical porosity count (based on ImageJ jPOR) results for the petrographic image taken from the Stephens 6 (6390'-6400') interval was estimated at 13% (Figure 4-6). There is a very good intercrystalline porosity along edges of equant dolomite rhombs (Figure 4-7). The EDS spectrum (Figure 4-8) exhibits a Mg^{2+} spike, with an approximate Ca/Mg ratio of 4 (84:19) (Table 4-4).

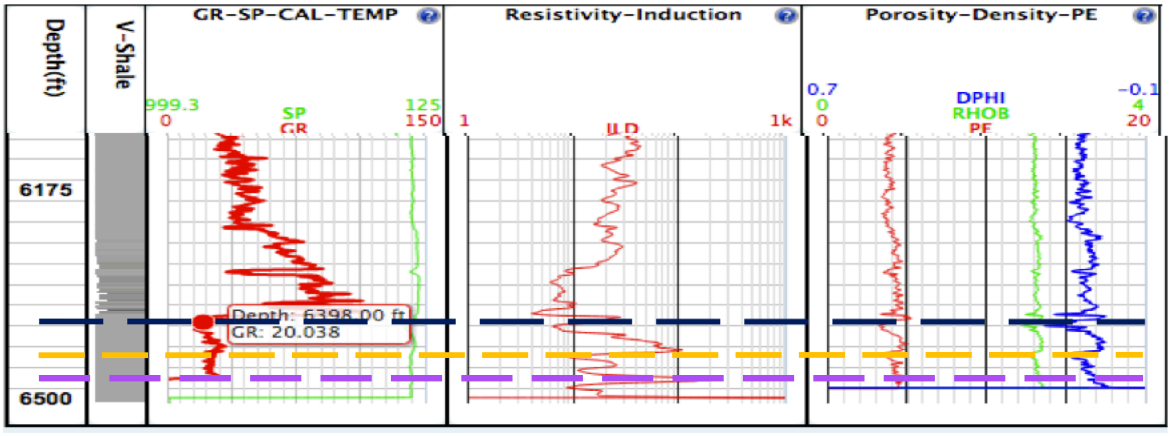

Figure 4-5. Viola Ls. top "A" Zone (in dark blue) "B" Zone top (in orange) "C" Zone top (in purple) for the Stephens 6 well.

Binocular Microscope Cuttings Description	Petrographic Microscope Thin Section Description	Total Estimated Porosity
Limestone cream grey lt grey, dense matrix, micro-cryptocrystalline; Chert cream off white, edge weathered, Dolomite sub-sucrosic to good rhombic development, scattered small vugs, overall fair-good interxln/vuggy porosity, even lt brown stain, poor shows	Dolomite with equant crystals dominant; Ooids and intraclasts more prevalent with interparticle porosity; presence of bryozoan noted; much more fossiliferous packstone- more mud-rich wackestone/packstone present; possible anhydrite present; minor packstone with muddy edges; pyrite present; minor chert present	13.2%

Table 4-3. Summary of cutting and thin section descriptions, as well as overall porosity percentage for the Stephens 6 well.

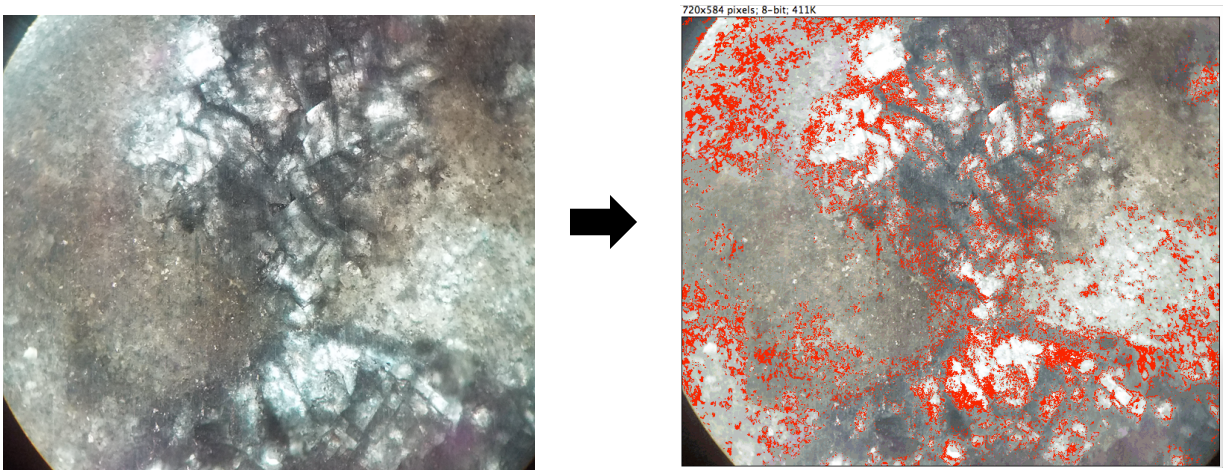

Figure 4-6. Optical PPL thin section image of the Viola Ls. in Stephens 6 well, and corresponding picture with isolated red color palette applied on the right to portray total porosity of 13.2%.

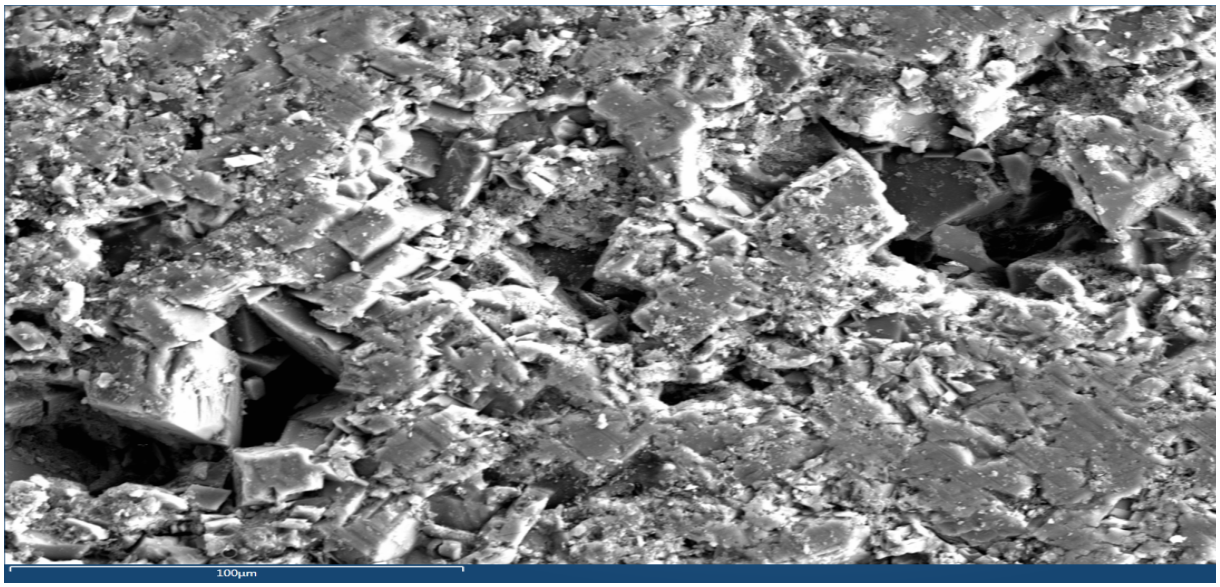

Figure 4-7. SEM DualBeam image at 100µm of Stephens 6 well, exhibiting intercrystalline porosity along dolostone rhombs.

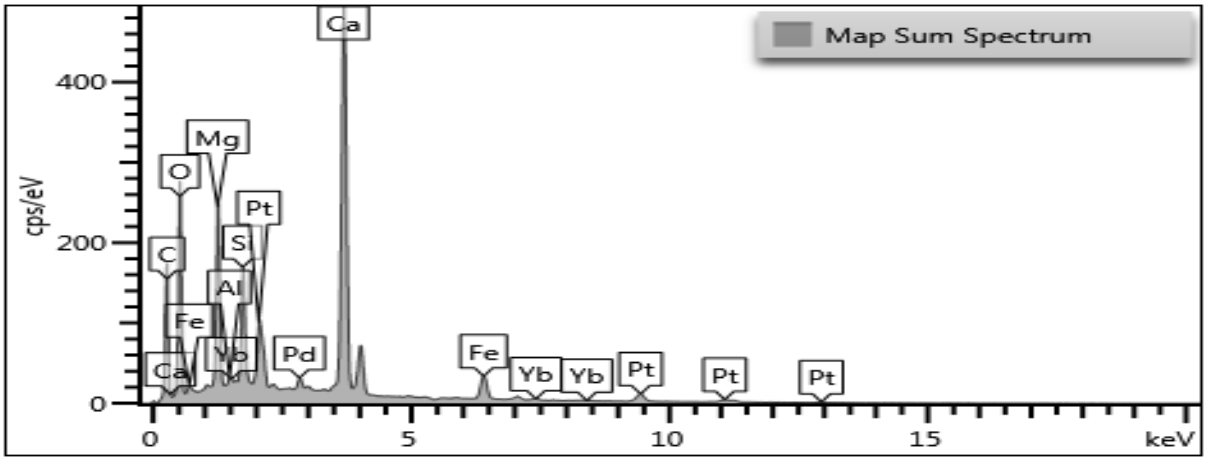

Figure 4-8. Graph of counts per section eV. Note spike in Ca/Mg depicted in map sum spectrum captured from Stephens 6 DualBeam image.

Element	Line Type	Apparent Concentration	k Ratio	Wt%	Wt% Sigma	Standard Label	Factory Standard
Ca	K series	84.92	0.75877	27.57	0.07	Wollastonite	Yes
Mg	K series	19.96	0.1324	9.11	0.04	MgO	Yes

Table 4-4. Summary of apparent concentrations and wt% of Ca/Mg, portraying spike in Ca/Mg for Stephens 6 well.

4.4 Stephens 9

Well cuttings were collected from where the Stephens 9 GAS well perforations target the Viola limestone at the (6450'-6480') interval with respect to the geologic report and well log, and were then analyzed using a binocular microscope (Figure 4-9). Under the binocular microscope, dense microcrystalline limestone and minor sucrosic textured dolostone, and some scattered chert were present. Thin sections from the same interval were then each analyzed using a petrographic microscope. The perforated interval mainly comprised of packstone/grainstone, oolitic limestone, chert, and minor subhedral limpid dolomite (Table 4-5). The Stephens 9 well target interval exhibits overall poor interparticle and interooid porosity. The total optical porosity count (based on ImageJ jPOR) results for the petrographic image taken from the Stephens 9 (6460'-6470') interval was estimated at 3% (Figure 4-10). There dolomite present in the Stephens 9 well perf zone exhibits less rhombic development with reduced surrounding void space (Figure 4-11). The EDS spectrum (Figure 4-12) exhibits a decline in Mg^{2+}, with an approximate Ca/Mg ratio of 80 (159:2) (Table 4-6).

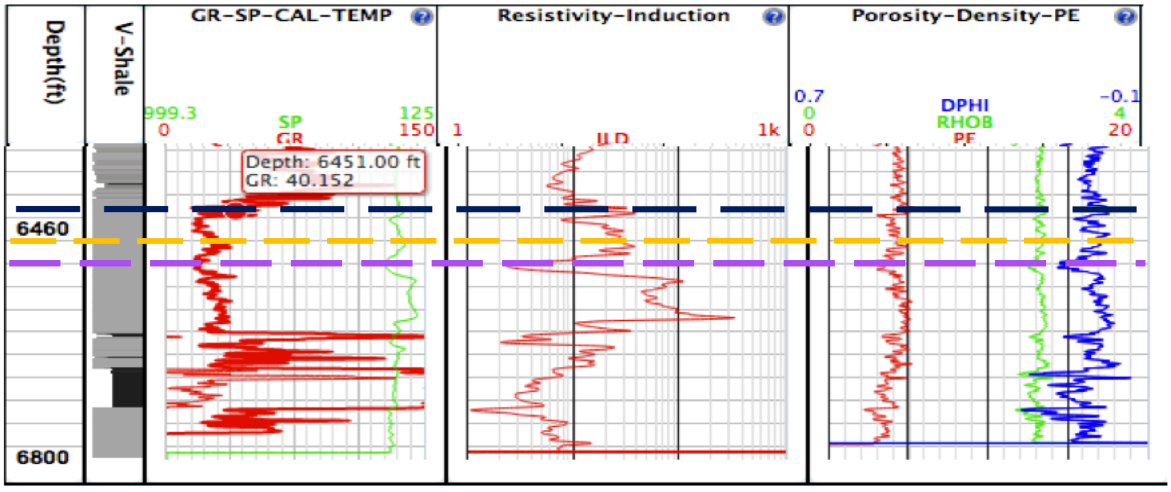

Figure 4-9. Viola Ls. top "A" Zone (in dark blue) "B" Zone top (in orange) "C" Zone top (in purple) for the Stephens 9 well.

Binocular Microscope Cuttings Description	Petrographic Microscope Thin Section Description	Overall Porosity
Limestone grey- lt grey some cream, dense and microcrystalline; sub-fossiliferous, some glauconitic in part, poor porosity, no shows; decrease in dolomite cream with overall good rhombic development and associated porosity, even golden brown stain, poor show oil; some scattered Chert: bone white, opaque, weathered, spotty edge stain	Packstone/grainstone dominant with ostracod, brach, and ooids; some presence of chert; not as much subhedral dolomite present; interooid porosity and minor fracture porosity along oolitic limestone; lots of hematite/siderite staining; some oil stain; very minor interparticle porosity	3.0%

Table 4-5. Summary of cutting and thin section descriptions, as well as overall porosity percentage for the Stephens 9 well.

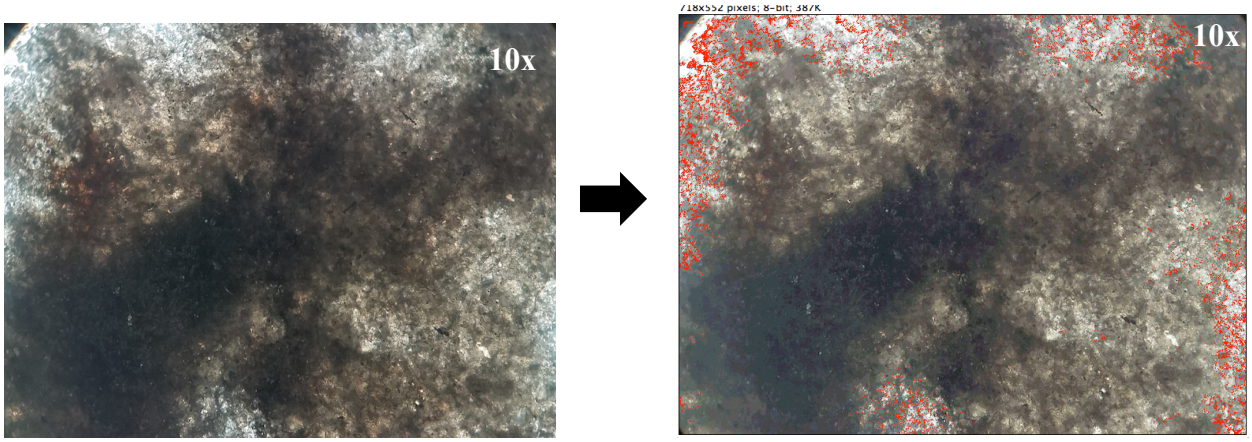

Figure 4-10. Optical PPL thin section image of the Viola Ls. in Stephens 9 well, and corresponding picture with isolated color palette applied on the right to portray total porosity of 3.0%.

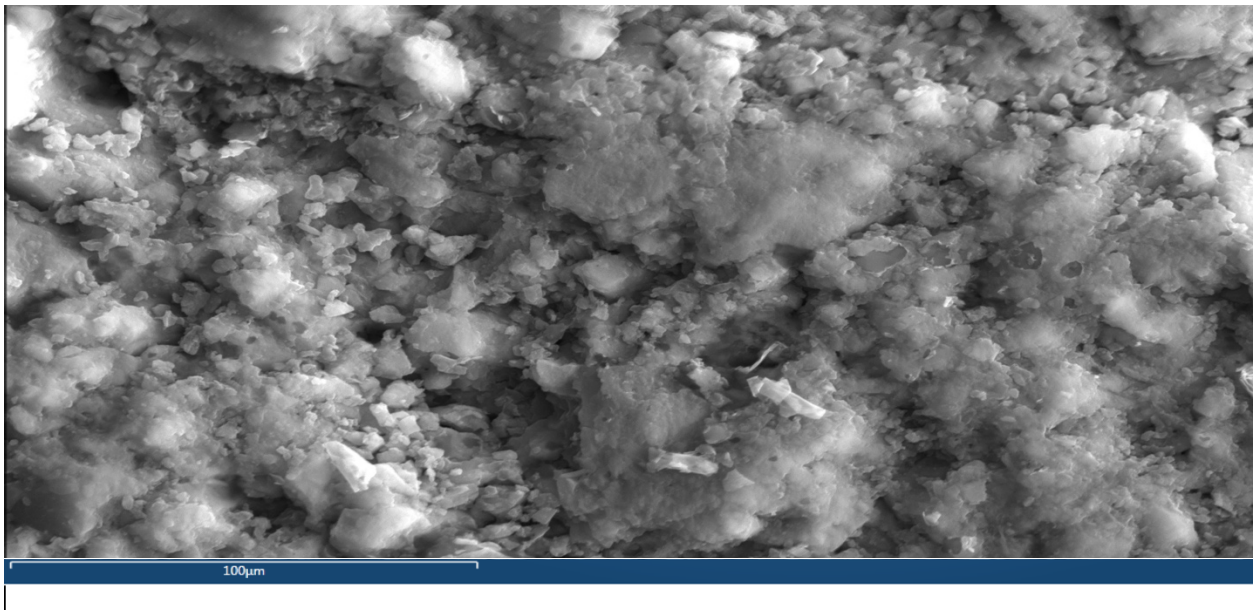

Figure 4-11. SEM DualBeam image at 100µm of Stephens 9 well, exhibiting minor void porosity along sub-equant dolomite rhombs and limestone.

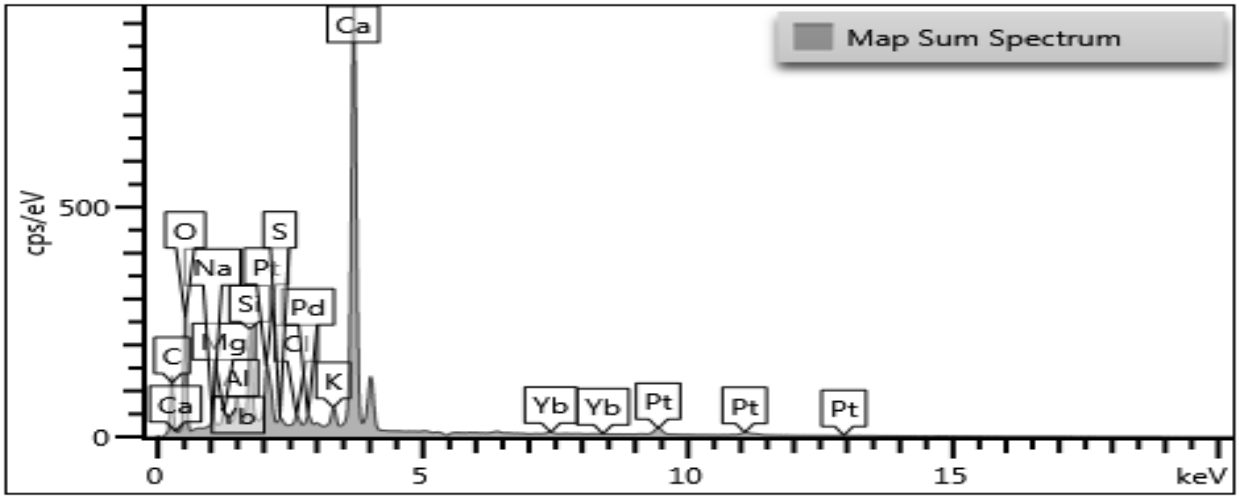

Figure 4-12. Graph of counts per section eV. Note decrease in Ca/Mg depicted in map sum spectrum captured from Stephens 9 DualBeam image.

Element	Line Type	Apparent Concentration	k Ratio	Wt%	Wt% Sigma	Standard Label	Factory Standard
Ca	K series	159.72	1.42711	38.06	0.08	Wollastonite	Yes
Mg	K series	2.31	0.01535	0.78	0.02	MgO	Yes

Table 4-6. Summary of apparent concentrations and wt% of Ca/Mg, portraying a decline in Mg^{2+} for Stephens 9 well.

4.5 Stephens 8

Well cuttings were collected from the Stephens 8 D&A well at the (6390'-6430') interval with respect to the geologic report and well log, and were then analyzed using a binocular microscope (Figure 4-13). Under the binocular microscope, dense microcrystalline limestone, minor sub-sucrosic textured dolostone, and very little chert were present. Collectively, this interval mainly comprised of intrasparite, some sucrosic subhedral dolostone, pyrite, and minor chert, when viewed in thin section (Table 4-7). The Stephens 8 well target interval exhibits overall poor to fair intercrystalline and interparticle porosity. The total optical porosity count (based on ImageJ jPOR) results for the petrographic image taken from the Stephens 8 (6449 c. 40 min.) interval was estimated at 5.7% (Figure 4-14). This interval predominantly consists of

limestone, with little to no porosity present within or along the limestone grains (Figure 4-15). The EDS spectrum (Figure 4-16) exhibits a slight drop in Mg^{2+}, with an approximate Ca/Mg ratio of 30 (120:4) (Table 4-8).

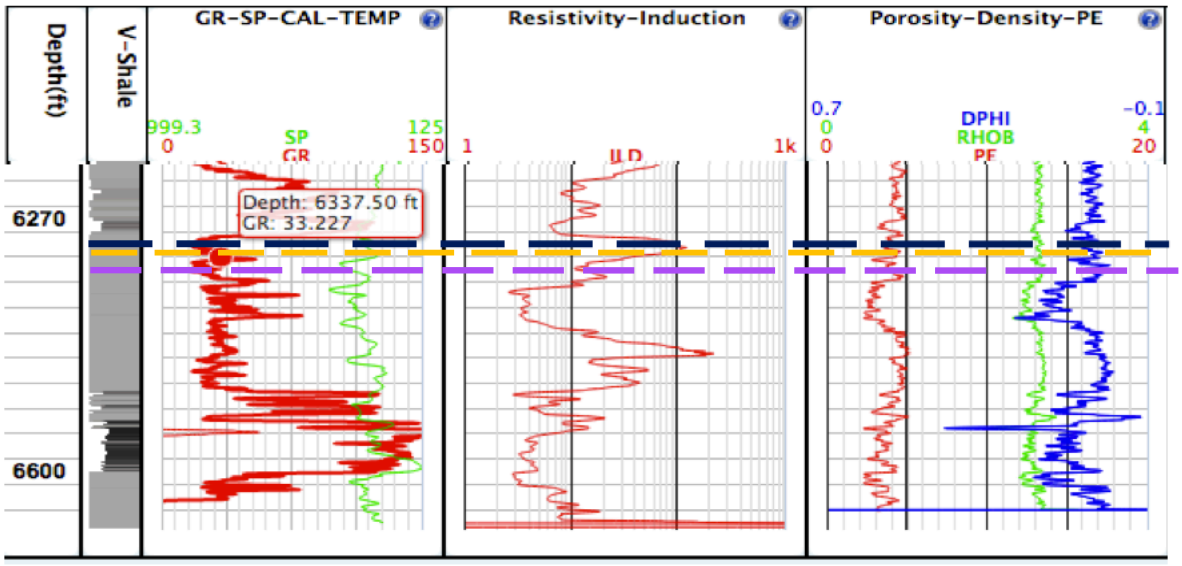

Figure 4-13. Viola Ls. top "A" Zone (in dark blue) "B" Zone top (in orange) "C" Zone top (in purple) for the Stephens 8 well.

Binocular Microscope Cuttings Description	Petrographic Microscope Thin Section Description	Overall Porosity
Limestone- cream, fossiliferous and mostly cryptocrystalline, marked decrease in chert and dolomite light grey to light tan, microcrystalline, sub-sucrosic, dens; chert is white to light grey, opaque, black speckled, some pyritic; no shows	Intrasparite limestone dominant; minor sucrosic subhedral dolostone; minor staining; very pyritic; minor clay; minor chert; some interparticle/intercrystalline and fracture porosity; minor intercrystalline porosity on dolostone	5.7%

Table 4-7. Summary of cutting and thin section descriptions, as well as overall porosity percentage for the Stephens 8 well.

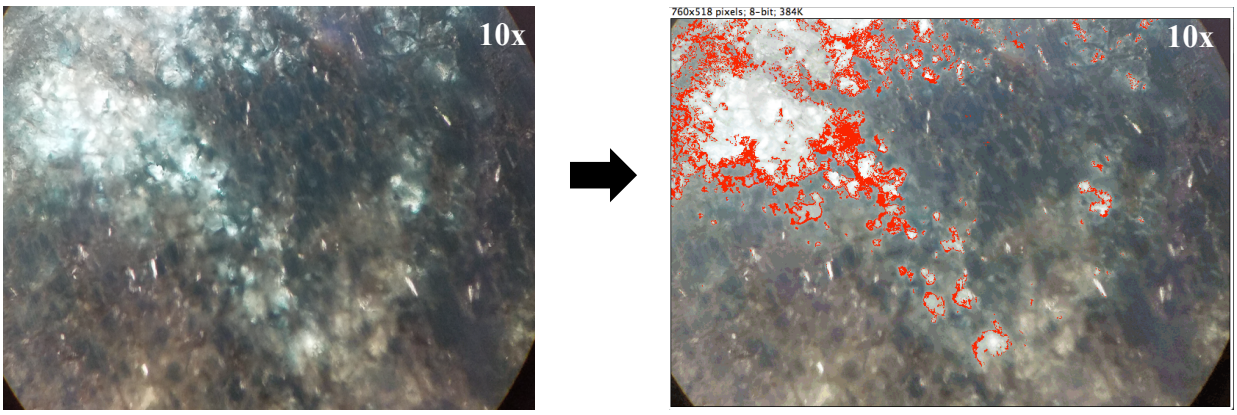

Figure 4-14. Optical PPL thin section image of the Viola Ls. in Stephens 8 well, and corresponding picture with isolated red color palette applied on the right to portray total porosity of 5.7%.

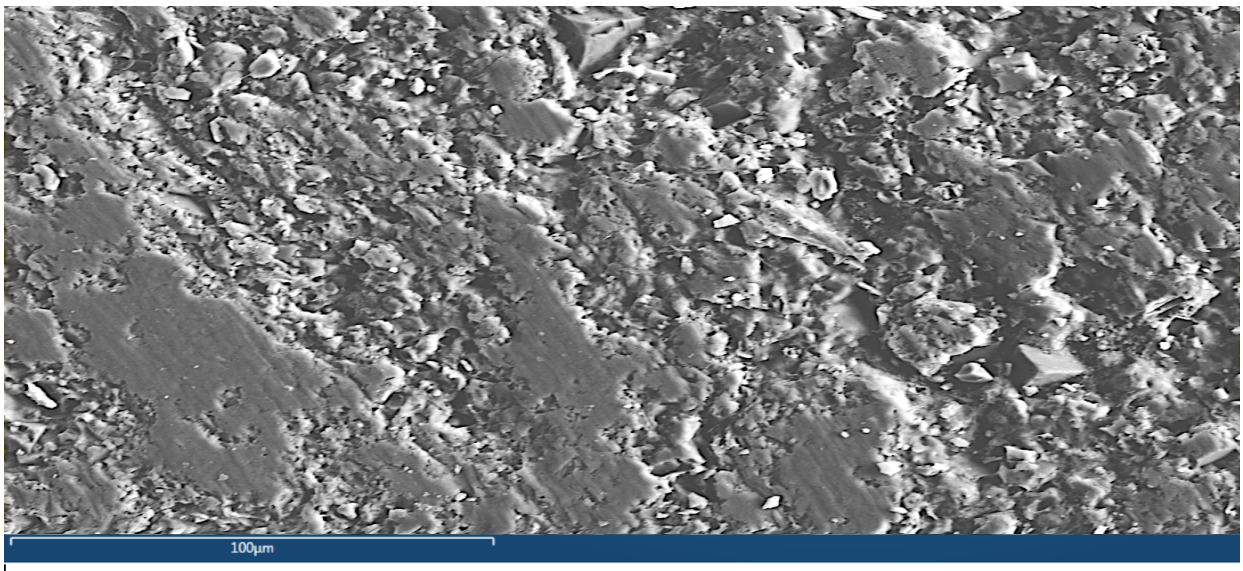

Figure 4-15. SEM DualBeam image at 100µm of Stephens 8 well, exhibiting poor porosity overall among limestone grains.

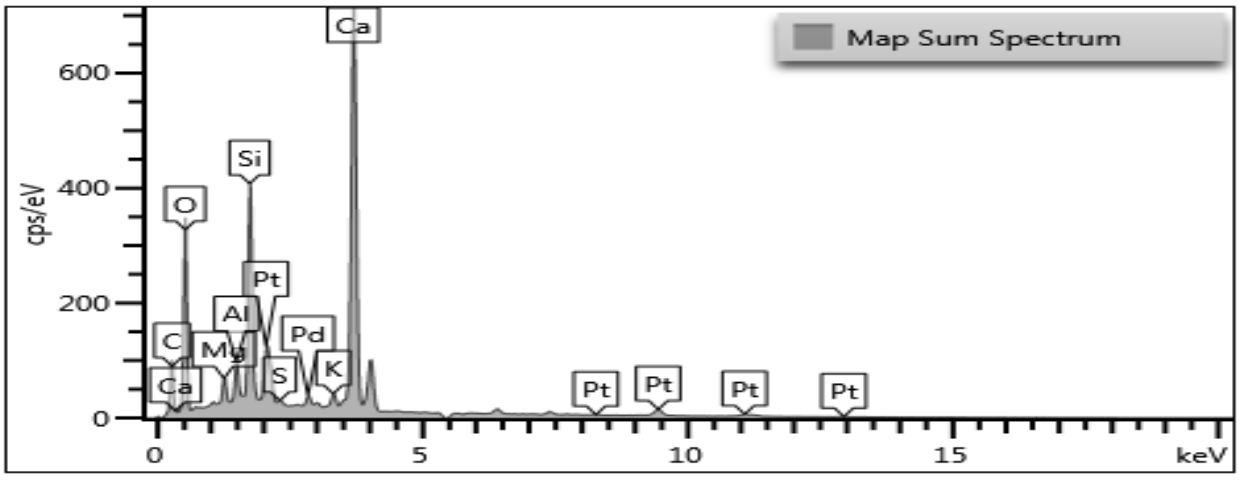

Figure 4-16. Graph of counts per section eV. Note slight decrease in Ca/Mg depicted in map sum spectrum captured from Stephens 8 DualBeam image.

Element	Line Type	Apparent Concentration	k Ratio	Wt%	Wt% Sigma	Standard Label	Factory Standard
Ca	K series	120.65	1.07798	30.82	0.08	Wollastonite	Yes
Mg	K series	3.99	0.02647	1.40	0.02	MgO	Yes

Table 4-8. Summary of apparent concentrations and wt% of Ca/Mg, portraying a decrease in Mg^{2+} for Stephens 8 well.

4.6 Stephens 3

Well cuttings were collected from the Stephens 3 D&A well at the (6420 c. 30 min.) interval with respect to the geologic report and well log, and were then analyzed using a binocular microscope (Figure 4-17). Under the binocular microscope, gray tabular shale and limestone were dominant, as well as an increase in chert and clay content, and a prominent decrease in dolostone. Collectively, this interval mainly comprised of shale, chert and packstone, while lacking in dolostone (Table 4-9). The total optical porosity count (based on ImageJ jPOR) results for the petrographic image taken from the Stephens 3 (6420 c. 30 min.) interval was estimated at 3.9% (Figure 4-18). This interval predominantly consists of limestone with very little intra/interparticle porosity along the grain edges (Figure 4-19). The EDS spectrum (Figure 4-20) exhibits a major decrease in Mg^{2+}, with an approximate Ca/Mg ratio of 160 (160:1) (Table 4-10).

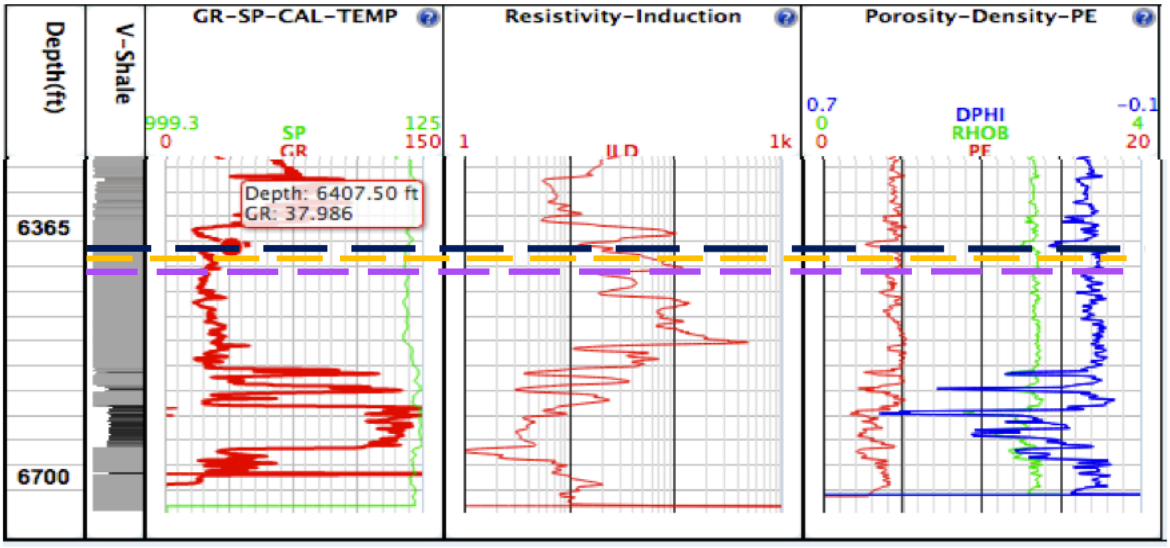

Figure 4-17. Viola Ls. top "A" Zone (in dark blue) "B" Zone top (in orange) "C" Zone top (in purple) for the Stephens 3 well.

Binocular Microscope Cuttings Description	Petrographic Microscope Thin Section Description	Overall Porosity
Grey tabular shale/limestone dominant; planar fractures in shale prominent; more red clay present; more (and huge) milky/bone white chert w/ very jagged edges present; not as much sucrosic dolomite present; still have a good bit of microcrystalline limestone (with minor staining); pyritic; no shows noted	Packstone dominant; prominent grey shale; minor dolomite present with subhedral rhombs; chert much more prevalent; prominent pyrite present; Very low porosity overall	3.9%

Table 4-9. Summary of cutting and thin section descriptions, as well as overall porosity percentage for the Stephens 3 well.

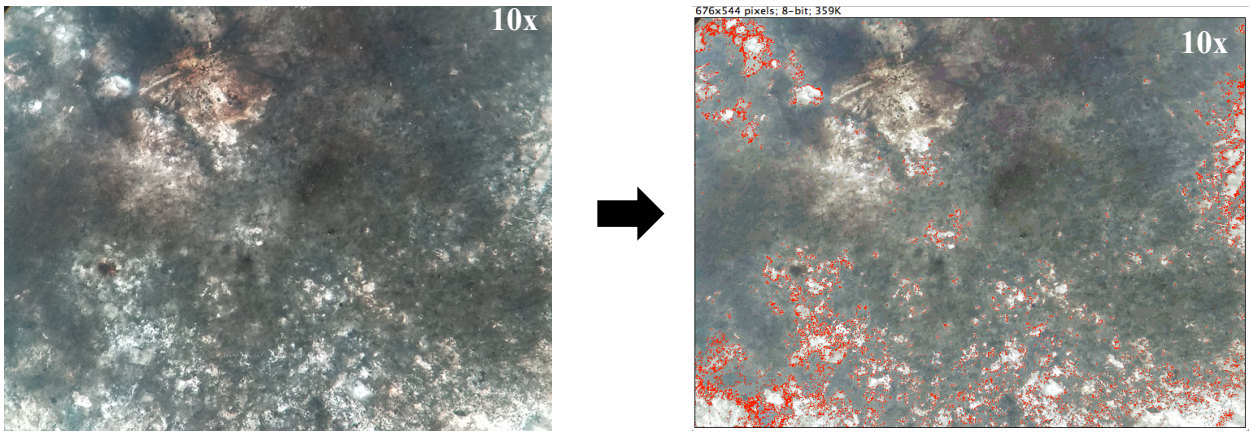

Figure 4-18. Optical PPL thin section image of the Viola Ls. in Stephens 3 well, and corresponding picture with red isolated color palette applied on the right to portray total porosity of 3.9%.

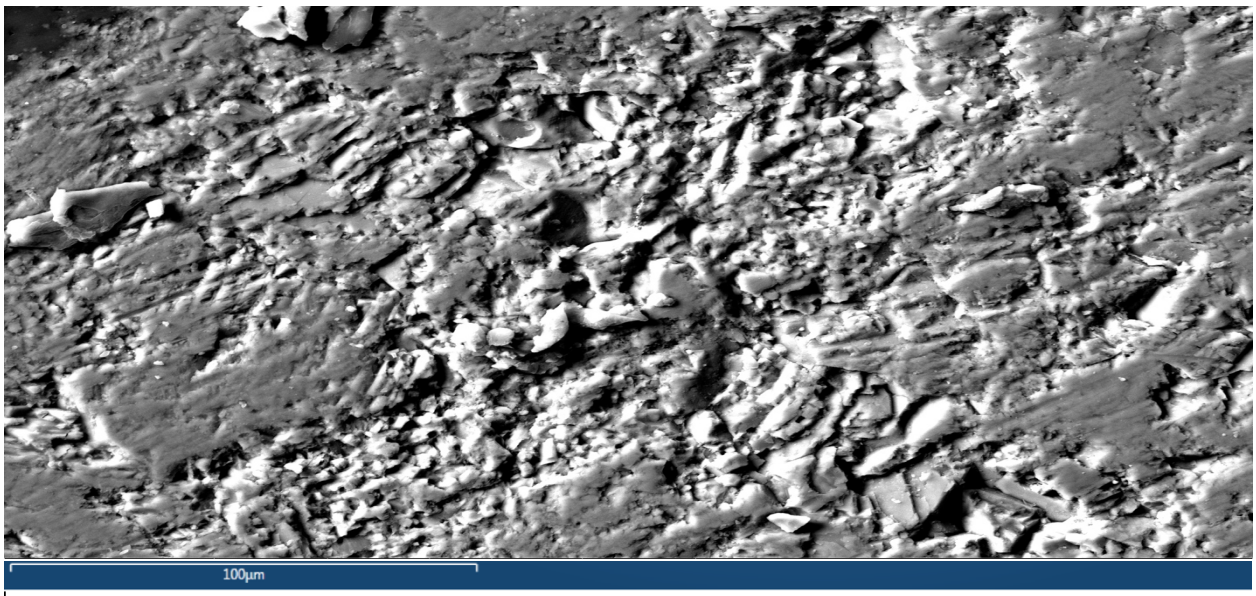

Figure 4-19. SEM DualBeam image at 100µm of Stephens 3 well, exhibiting very poor porosity overall among limestone grains.

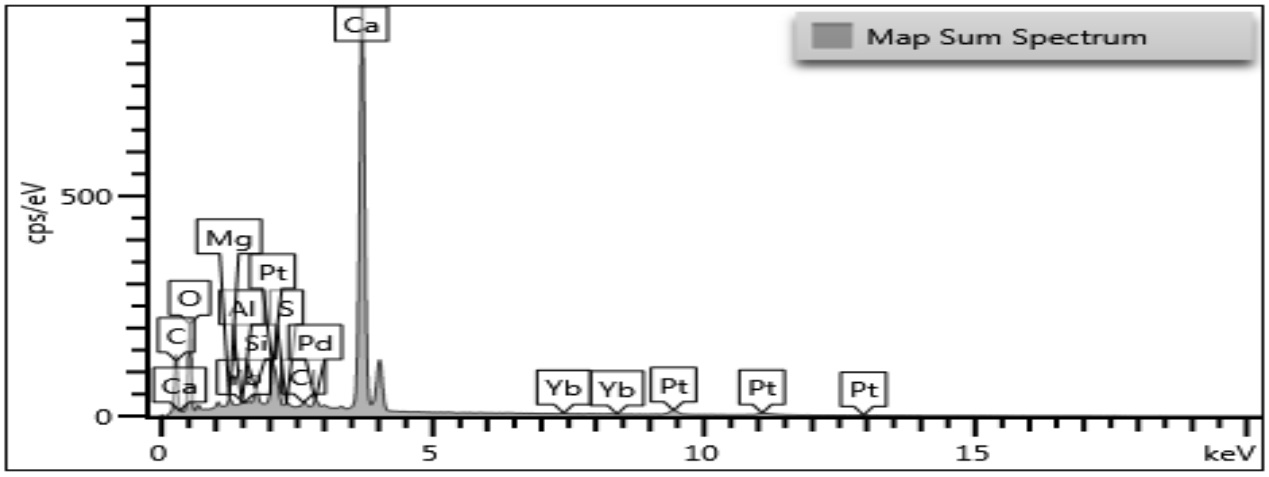

Figure 4-20. Graph of counts per section eV. Note major decrease in Ca/Mg depicted in map sum spectrum captured from Stephens 3 DualBeam image.

Element	Line Type	Apparent Concentration	k Ratio	Wt%	Wt% Sigma	Standard Label	Factory Standard
Ca	K series	159.31	1.42337	44.99	0.12	Wollastonite	Yes
Mg	K series	1.30	0.00860	0.55	0.02	MgO	Yes

Table 4-10. Summary of apparent concentrations and wt% of Ca/Mg, portraying a significant decrease in Mg^{2+} for Stephens 3 well.

4.7 Results Summary

The following table and graph of the five examined wells shows the new Ca/Mg ratio and total porosity (%) data collected as part of this study, and how these parameters correspond to current oil and gas production rates (Table 4-11, 4-12). Further thin section images are available in Appendix B.

Well Name	Current Production Status	Years of Production	Oil production (bbls)	Gas production (mcf)	Ca/Mg	Total ϕ (%)
Stephens 4	O&G	2012 2013 2014 2015	46430 18,113 11,151 2,286	0 0 0 0	3:1	20.5%
Stephens 6	O&G	2013 2014 2015	6,701 1,608 306	10,938 4,506 1,709	4:1	13.2%
Stephens 9	O&G	2013 2014 2015 2016	0 124 0 0	3373 155,408 90,217 19,162	80:1	3.0%
Stephens 8	D&A	2013	0	0	30:1	5.7%
Stephens 3	D&A	2011	0	0	160:1	3.9%

Table 4-11. Summary of the correlation between production status, rates of production, Ca/Mg, and total porosity for wells of interest.

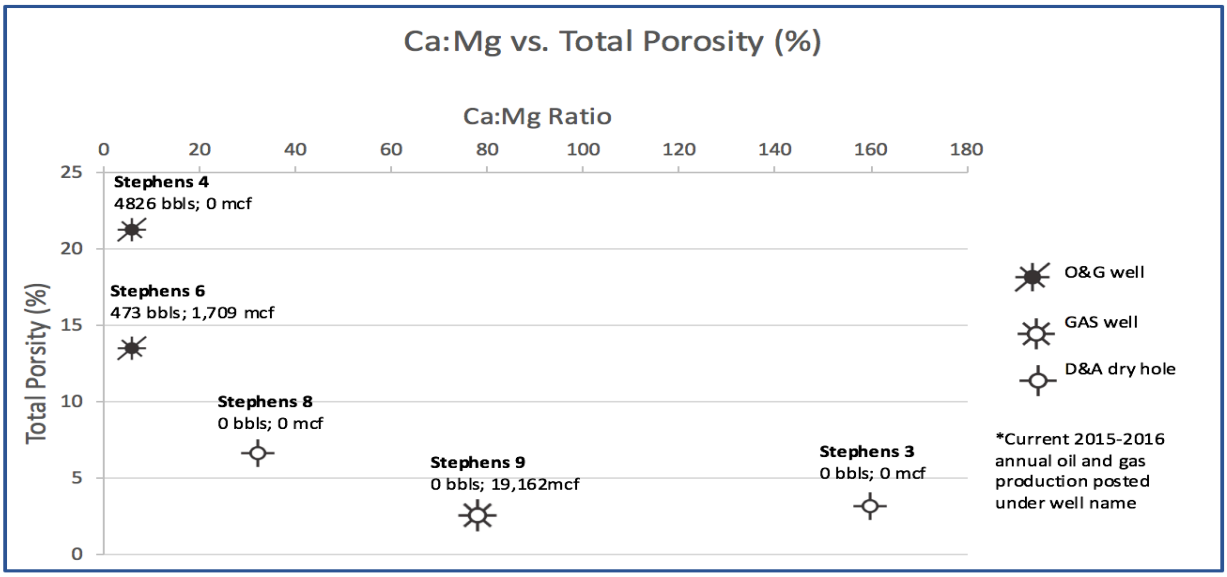

Table 4-12. Plotted correlation of Ca/Mg vs. Total Porosity (%) for wells of interest.

Chapter 5 - Discussion

5.1 Structure

A Viola limestone structure map was generated on Petra across the T32S-R1W study area (Figure 5-1). The top of the Viola Ls. structure can be seen across the Morrison Northeast field, outlined in black. The map shows a gentle sweeping structure for the Viola formation when trending across the field area, further indicating a lack of structural control. A structural cross-section was generated based on the well-log correlation of the Stephens 9, Harden 1, Stephens 7 and 5 wells, in order to exhibit the lateral variations in thickness of the Viola trending from west to east (Figure 5-2).

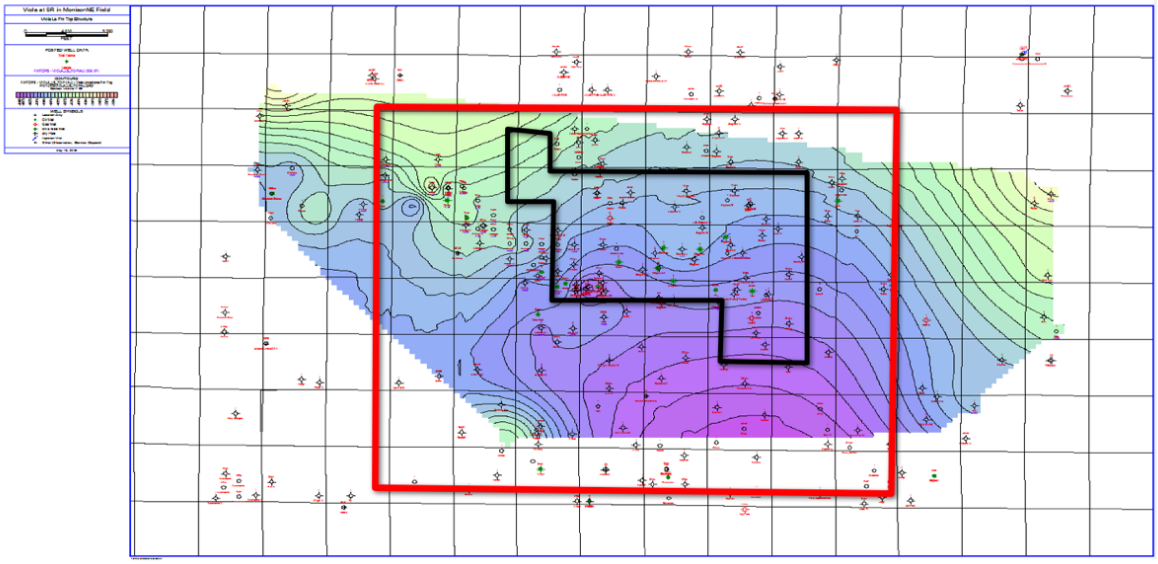

Figure 5-1. Structure map of the Viola Ls. with Morrison Northeast field highlighted in black.

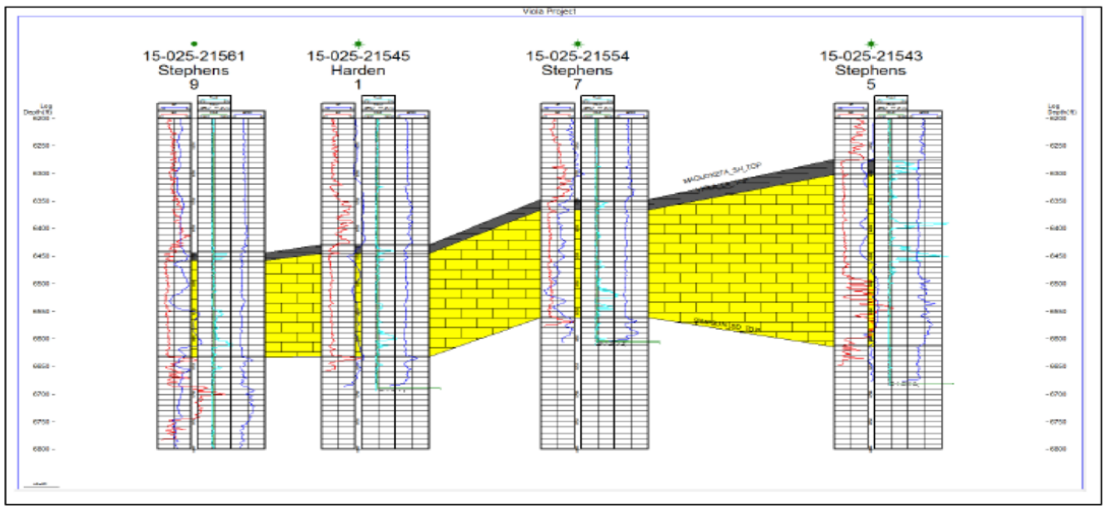

Figure 5-2. Structural cross-section of the Maquoketa Sh. And Viola Ls. formation tops seen in the Stephens 9, Harden 1, Stephens 7 and Stephens 5 wells.

5.2 Lithofacies Interpretation

Only the upper two "A" and "B" Zone facies were examined in detail for lithofacies interpretation, since they were the predominant lithofacies observed in the perforation zone across all of the Stephens Ranch wells. The "A" Zone facies exhibits a high modal abundance of chert and dolostone with well-developed equant-planar rhombic crystal morphologies, whereas the "B" Zone facies is primarily composed of wacke/packstones with a noticeably lower proportion of euhedral rhombic dolostone and less chert. When comparing the hydrocarbon production across the field, there was a distinguishing difference between which facies were present in each of the well's perforation zone. The aforementioned producing wells, Stephens 4, 6 and 9, all exhibited a notable presence of well-developed rhombic dolomite. The D&A wells, such as Stephens 3 and 8, both exhibited a higher percentage of wacke/packstones, while lacking in euhedral dolomite. This significant difference is seen between the "A" Zone and "B" Zone facies, which further suggests that the process of dolomitization may play a critical role in the difference in production that has been seen across the Stephen's Ranch lease in the Morrison Northeast field.

5.3 Stages of Diagenesis

Depositional processes serve as the starting foundation for the carbonate rock's original framework facies and primary pore space. While the rock facies' textural and granular framework initially models the depositional environment, it is the process of diagenesis that ultimately governs the rock's chemistry, texture and potential for fluid flow (Syed et al., 2010). The stages of diagenesis (eogenesis, mesogenesis, and telegenesis), which are otherwise known as the paragenetic sequence, will dictate the threshold or window for the various conditions and chemical changes that are initiated throughout the rock's burial history (Figure 5-3) (Murray and Pray, 1965). In the case of carbonates, the stage of regional diagenesis is limited to a narrow window of time in a restricted shallow marine environment, where the sediment is exposed to changes in pressure and temperature, and additionally subjected to metasomatic fluids (Syed et al., 2010). The process of carbonate diagenesis generally involves burial, compaction, replacement, fracture fill, and in some cases, dolomitization occurring, all either instantaneously or in successive order (Murray and Pray, 1965).

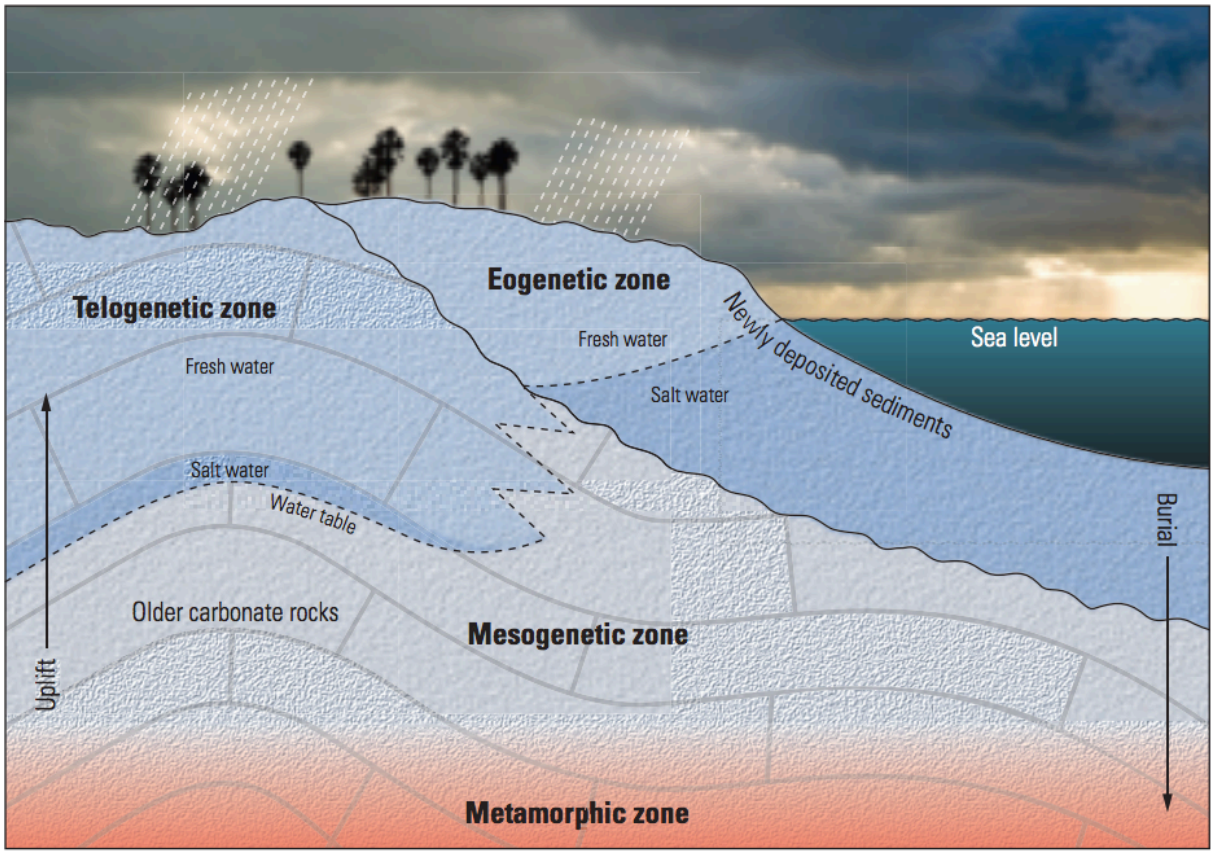

Figure 5-3. This diagram shows the various stages of the paragenetic sequence and where they occur relative to depth to the surface (Syed et al., 2010).

The first stage of diagenesis, which is known as eogenesis, takes place syn- to post-deposition in a shallow-burial environment (Syed et al., 2010). The onset of eogenesis occurs when the deposited limestone is exposed to shallow surface conditions. With the progression of burial, pressure and temperature, along with the introduction of metasomatic fluids, which then begin to chemically alter the rock (Syed et al., 2010). With continued burial and compaction, mineral replacement of calcite cement will start to occur, resulting in a significant decrease in porosity due to the presence of carbonate and/or evaporitic mineral replacement of the cement matrix (Syed et al., 2010).

The middle stage of diagenesis is mesogenesis, which can only occur when the rock is buried deeper, beyond a threshold of 2 km (Syed et al., 2010). Dolomitization begins to take

place from the early onset of mesogenesis to late stage telegenesis, as meteoric fluids are introduced to the exposed formation (Anastasiu and Dumitru-Relu, 2009). Evidence of mesogenesis includes pronounced cementation and recrystallization of calcite to dolomite, as well as the onset of partial dissolution (Welch, 2001).

If carbonates undergo the last stage of diagenesis, which is known as telegenesis, it will occur when the rock formation has been buried for a long period of time in regional settings where mountain building events and erosional events begin to take place (Syed et al., 2010). An unconformity present in deeply-buried rocks can serve as a barrier marking the separation of middle to late-stage burial diagenesis (Syed et al., 2010). Petrographic evidence that suggests that telegenesis has taken place includes the dramatic increase in secondary porosity due to the presence of dolomitization and the continued compaction and fracture fill (Syed et al., 2010).

In regards to the "A and B" Zone facies of the Viola limestone, noticeable stages of the paragenetic sequence can be seen when examining the thin sections. Evidence of early to late diagenetic alterations having occurred to the Viola limestone facies include the presence of dolomitization, stylotization, mineral replacement of sulfide and iron (III) oxide minerals, with continued compaction and fracturing when subjected to the subsequent burial conditions (Table 5-1) (Syed et al., 2010). All of the thin sections from both of the "A and B" Zone facies exhibited visible signs of early to middle stage paragenesis, indicating that eogenesis and possibly mesogenesis occurred prior to a major erosional event, when the Viola limestone was still buried in a shallow near-surface setting (Syed et al., 2010). As seen in the thin sections for this study, early stages of cementation reducing the primary porosity were evident in most thin sections (Syed et al., 2010). Some of the thin sections exhibited middle stage alterations with the presence of dolomitization, production of iron-rich minerals, such as hematite staining, as well as the

presence of pyrite nodules, and other opaque minerals. Alongside the new metastable minerals, the existence of fracturing having occurred along or in between the grains also signifies that the Viola limestone has been exposed to some middle to late-stage diagenetic alterations.

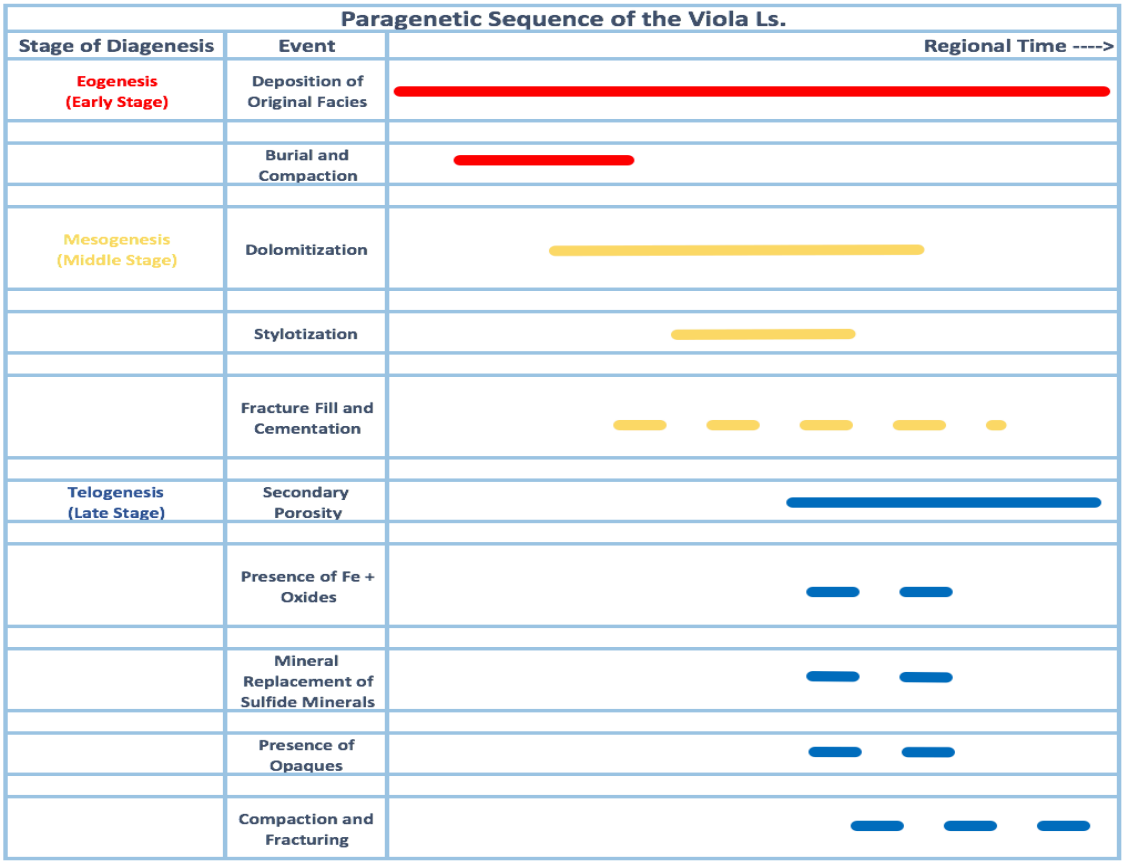

Table 5-1. Paragenetic sequence of the chronologic events that occurred as the Viola Ls. underwent burial; red indicates early stage shallow-burial, yellow indicates middle stage burial, and blue indicates late stage deep-burial.

5.4 Dolomitization Models

The most important process to take place in the paragenetic sequence of carbonates is dolomitization (Welch, 2001). Dolomitization is one of the longest and most variable diagenetic processes that can occur in successive stages, starting from shallow-surface to deep-burial, resulting in variable phases of dolomitization seen across subsequent lithofacies (Warren, 2000). In the case of the Viola limestone in the Morrison Northeast field, the "A" Zone facies showed notable petrographic signs of dolomitization occurring from the seepage-reflux model, while the underlying "B" Zone facies displayed a more diagnostic case for "Dorag" mixing-zone dolomitization. Both major dolomitization models are exhibited between the adjacent "A" Zone and "B" Zone facies. This is due to the various factors that favor each scenario, most notably the facies' water depth and water chemistry (Warren, 2000).

The "B" Zone facies contains no evaporites, in either cutting or thin section, indicating that this particular facies of the Viola Ls. was exposed syndepositionally in a shallow shelf-edge environment that was flooded by both marine and meteoric waters (Warren, 2000). Since the "B" Zone facies is not associated with a hypersaline seawater setting, it can be presumed that this facies was dolomitized from "Dorag" mixing-zone processes (Warren, 2000). This "Dorag" model is a classical case used to explain dolomitization having occurred without the presence of evaporitic minerals (Figure 5-4) (Warren, 2000). During burial, the "B" Zone facies continued to be flushed with fluids, resulting in pore-water meteoric leach (Warren, 2000). The meteoric leach then dissolved the non-matrix cement, resulting in moldic-filling of the pore space (Welch, 2001). Further indications of a "Dorag" model for the "B" Zone facies, includes the prominent occurrence of non-marine-type deposits, such as lacustrine shale and mudstone, as well as the presence of intrasparite, rather than skeletal allochems (Warren, 2000).

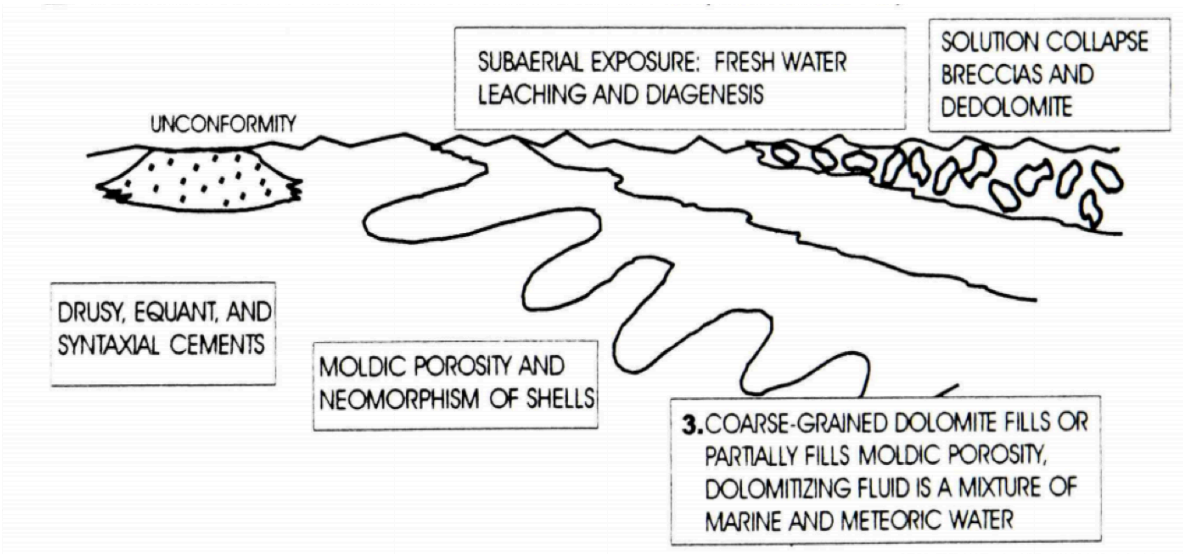

Figure 5-4. "Dorag" mixing-zone dolomitization model for "B" Zone facies (Welch, 2001).

Conversely, the thin section samples from the top "A" Zone lithofacies contain evaporitic minerals, particularly anhydrite. This suggests that the top lithofacies of the Viola was dolomitized during a period of sub-aerial exposure, due to hypersaline seepage-reflux (Figure 5-5) (Warren, 2000). Seepage-reflux dolomitization can occur when Mg^{2+}-rich seawater saturates the formation matrix, altering the trapped connate fluids in the sediment, augmenting the rhombic development of dolomite, and consequently enhancing the matrix-selective intercrystalline and interparticle porosities (Welch, 2001). Both types of porosity are prominent in the "A" Zone facies, while minor or lacking in the underlying "B" Zone (Welch, 2001).

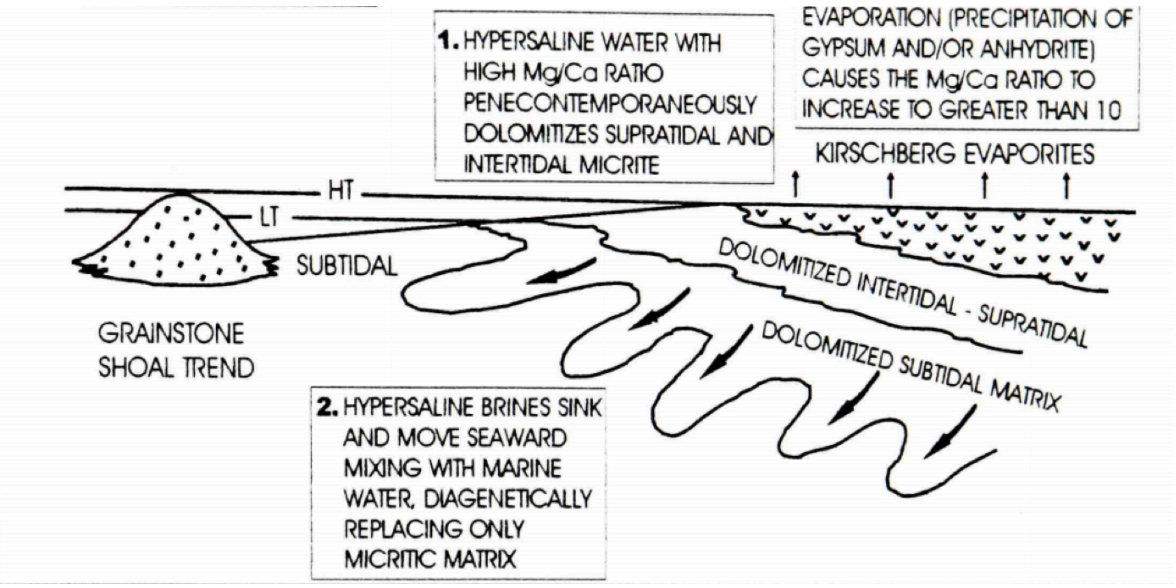

Figure 5-5. Seepage-reflux dolomitization model for the "A" Zone facies (Welch, 2001).

Hypersaline brine is much more abundant in Mg^{2+}, yielding a higher Ca/Mg ratio in lithofacies that have undergone seepage-reflux dolomitization (Warren, 2000). As noted earlier, the top of the Viola's "A" Zone facies was deposited in an intertidal to supratidal environment with cyclic transgression-regression events, leading to evaporation precipitation that is diagnostic of seepage-reflux dolomitization (Warren, 2000). The producing Stephens 4, 6 and 9 wells were all perforated in the "A" Zone facies, correlating to the aforementioned spike in Mg^{2+}. In contrast, the dry Stephens 3 and 8 wells exhibited a lower Ca/Mg, indicative of the "B" Zone facies. This difference in Mg^{2+} concentrations is evident when comparing the dolomite between the "A and B" Zone facies in the Viola Ls., further illustrating an image of two dolomitization models occurring between two adjacent lithofacies, further isolating the more productive zone (Figure 5-6).

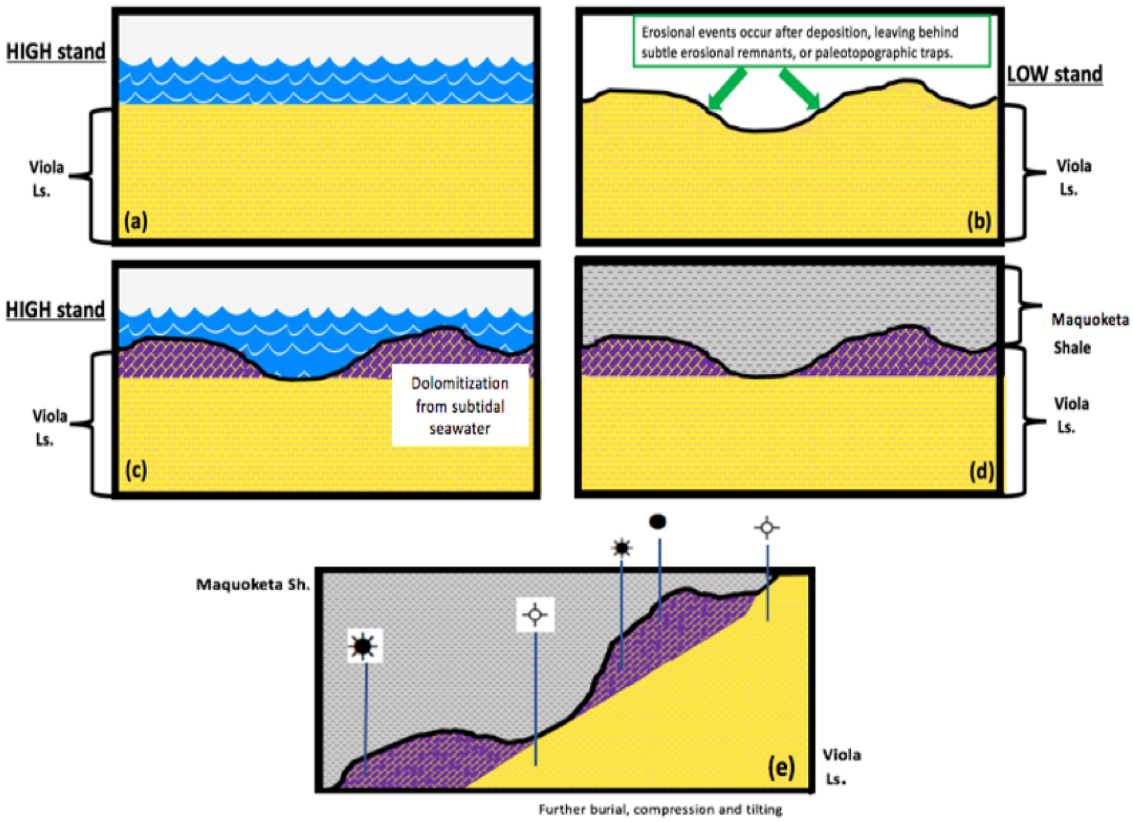

Figure 5-6. Illustration representing dolomitization processes: (a Viola deposits at HS, followed by (b) deposition at LS with subsequent erosion, (c) successive periods of HS, facilitating dolomitization to preserved erosional remnants of the Viola (in purple), (d) deposition of the Maquoketa Sh., and (e) further burial, compression and tilting of the Viola Ls. showing wells and how production correlates to well placement.

The "A" Zone facies exhibits favorable reservoir conditions, such as higher concentrated Mg^{2+}- dolomite and prominent intercrystalline porosity. Furthermore, the "A" Zone sits at the top of the Viola Ls., which has made it more susceptible to middle to late-stage diagenetic alterations, such as continued compaction and fracturing, enhancing the secondary porosity (Syed et al., 2010). Additionally, by causal sequence, the top of the Viola sits unconformably below the Maquoketa shale, providing a stratigraphic trap for areas where there are paleotopographic erosional remnants of the "A" Zone (Richardson, 2013). The development of these elevated "paleotopographic highs" appears to serve as seals along the flanks of the "A" Zone lithofacies, potentially isolating the productive strata. The 3D seismic attribute analysis will

now be examined in order to ground truth the stratigraphic heterogeneities that are controlling the Viola's hydrocarbon production.

5.5 Lithofacies to Seismic Facies Correlation

To determine which wells exhibit optimal well placement, a 3D seismic attribute analysis was performed to determine exactly which reservoir parameters are needed to delineate where the highest hydrocarbon production is. In order to conduct a reservoir characterization of the target Viola Ls., it was pertinent for the Viola to be analyzed as a series of seismic horizons, in order to dissect the seismic wavelet's peaks and troughs that denote the lateral and vertical variations of the Viola across the seismic survey (Raef et al., 2016). The seismic facies were extracted on the basis of various seismic attributes, in order to establish the clear-cut signatures of each horizon. The seismic attribute workflow ultimately consisted of various attributes that isolated velocity anomalies across the Viola horizon picks (Raef et al., 2016). The best 3D seismic attributes that can be applied to carbonates, include the following: instantaneous phase, normalized amplitude, instantaneous frequency and thin bed indicator (Raef et al., 2016). Since horizon tracking and applied seismic attribute analysis is an integral part to prospect evaluation, each attribute had to be exclusively applied to see which one exhibited the finest resolution of the lateral stratigraphic variations of the Viola beds, as well as the thickening and thinning of the beds across the field (Raef et al., 2016).

After examining each of the individual seismic attributes, it was gathered that the attributes that revealed the most prominent resolution of the varying thickness of the Viola beds, were the instantaneous attributes, such as instantaneous frequency and thin bed indicator (Raef et al., 2016). The thin bed indicator attribute was able to clearly define the lateral heterogeneities

that are characteristic of the upper Viola seismic facies. When applied, these instantaneous attributes were able to collectively resolve the boundaries between the seismic facies by causing an increase in the resolution of the seismic doublets that were indicative of the thinning and thickening of the Viola beds (Figure 5-7) (Raef el al., 2016). The only way these seismic doublets were able to be extracted is by the presence of a low velocity anomaly (Raef et al., 2016). In the case of subsurface formations, low velocity anomalies can occur either due to a presence of highly porous rocks or from a lower impedance caused by the presence of hydrocarbons.

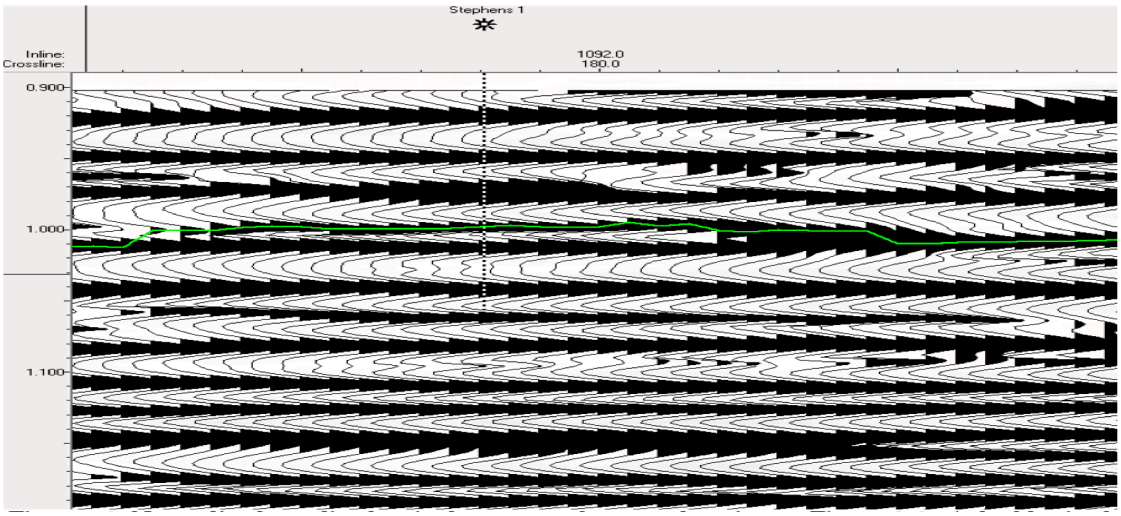

Figure 5-7. This figure portrays horizon tracking (in green) of the Viola Ls. seismic doublets. Notice lateral variations exhibited by peaks and troughs. (Raef et al, 2016).

After determining that these seismic doublets were indicative of increased production, the next step was to determine which wells had seismic doublets present near the borehole. At this point, the normalized amplitude attribute played a critical role in detecting well placement in correlation to these seismic doublets that were visible after an intensified instantaneous frequency with an instantaneous decrease in amplitude. These attributes resolved where there were thin bed indicator peaks in conjunction with lower amplitude anomalies along the "A" Zone

horizon track and amplitude maps, allowing for proper identification of productive well placement (Raef et al., 2016) (Figure 5-8). In effect, the reservoir quality seismic facies correlate to the dolomitized portion of the paleotopographic trap within the upper facies of the Viola. Ultimately, this created a stratigraphic trap that isolates where the productive zone is, further supporting that the rocks control production rather than structure (Figure 5-9).

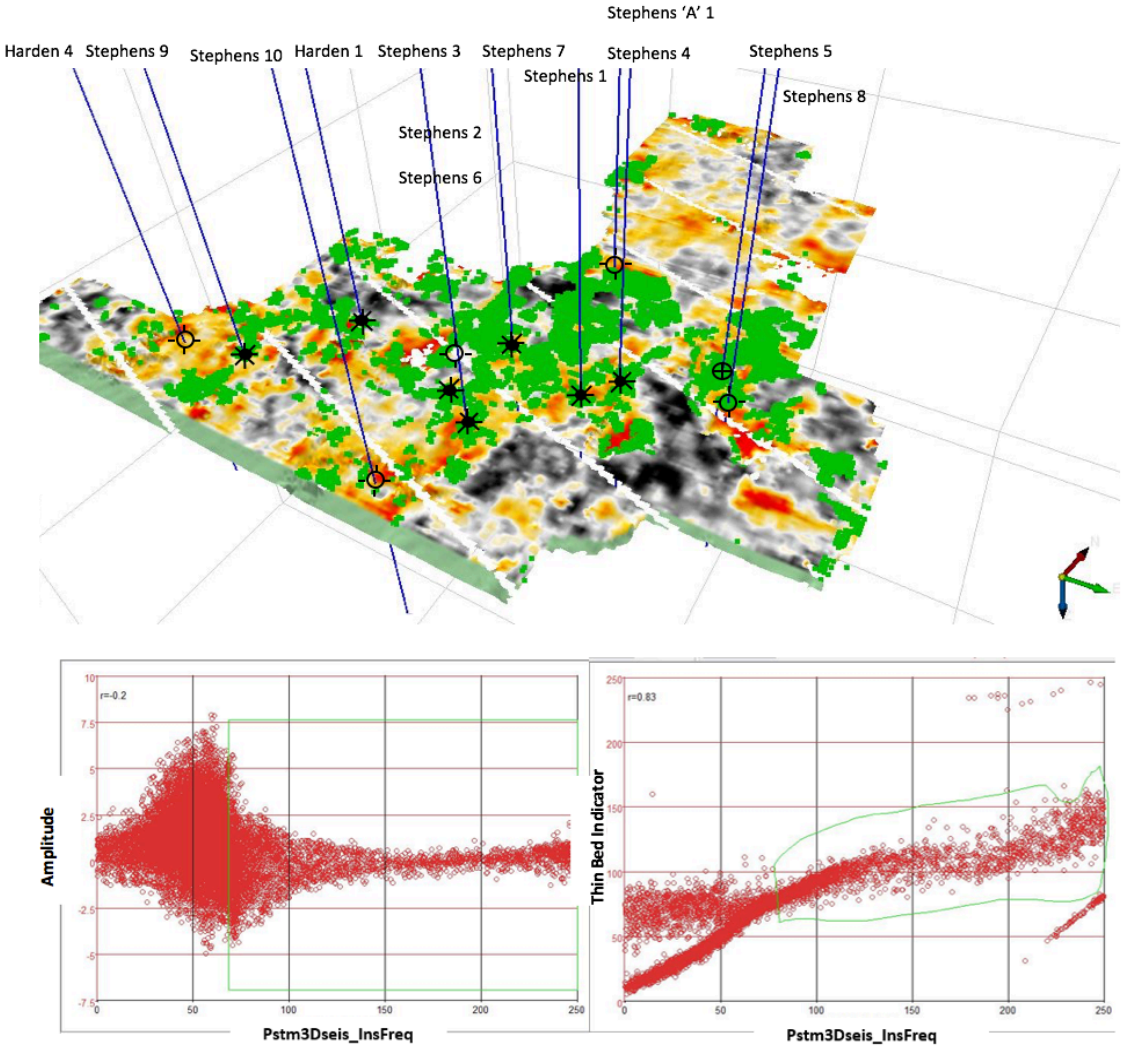

Figure 5-8. Time structure map of survey area with corresponding chart of normalized amplitude and thin bed indicator attributes. The producing O&G wells are denoted (in black) plot on the green area of the map, while most D&A wells (in open circle) plot on the white and red areas of the map. The producing wells correspond to areas of high thin bed indicators where there are also low amplitude anomalies (Raef et al., 2016).

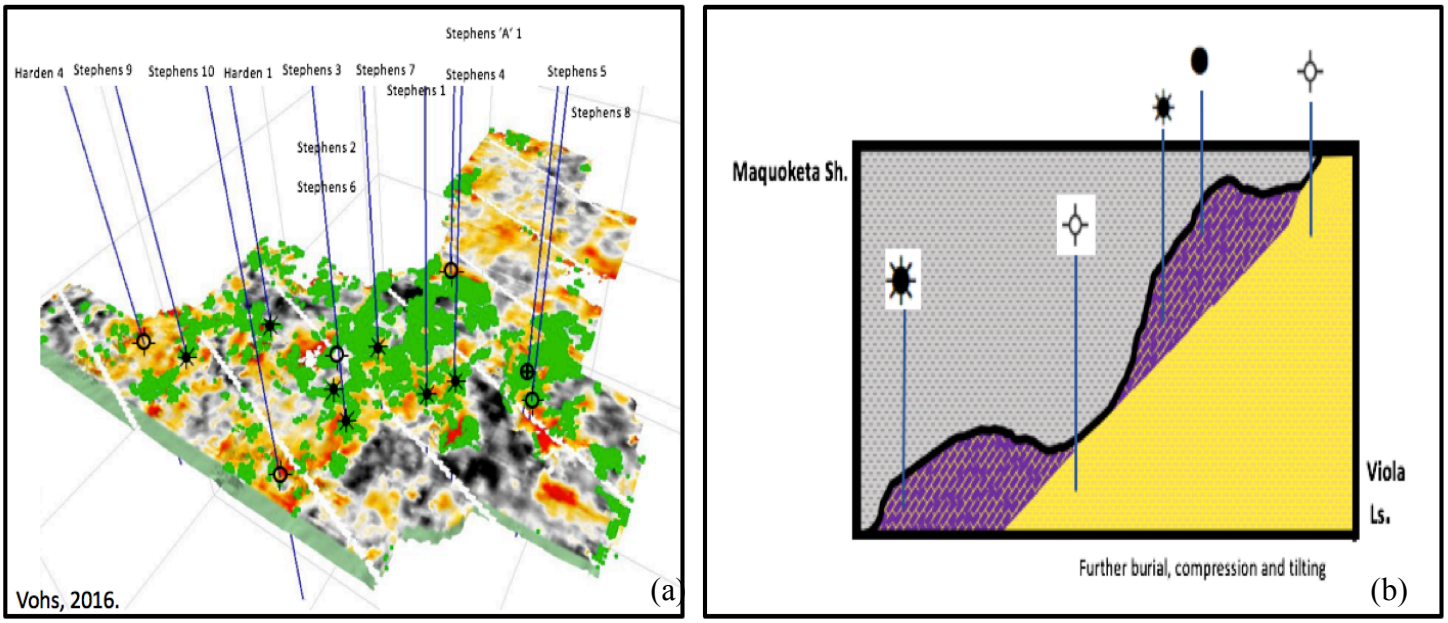

Figure 5-9. Illustration of (a) seismic attributes stratigraphically delineate (in green) where the seismic facies correlates to (b) the dolomitized portion of the paleotopographic trap within the upper facies of the Viola; creating a stratigraphic trap (in purple) (Raef et al., 2016).

Chapter 6 - Conclusion

The Middle Ordovician-aged Viola limestone is the primary target formation in the Morrison Northeast Field of Clark County, Kansas. Past and current production out of the Viola Ls. has been rather unpredictable in the Morrison Northeast Field, due to a lack of structural control. Evaluating other hydrocarbon entrapment mechanisms for this field has allowed for a more detailed look into the borehole lithology of the Stephens Ranch wells that are currently being operated by Coral Coast LLC. Using the provided well data and available drill-cuttings, a petrographic study of the lithofacies was combined with a 3D seismic attribute analysis were both conducted in order to determine optimal well placement to target the Viola.

A total of eleven wells in the Stephens Ranch lease were investigated; with only five yielding results. The Stephens 4, Stephens 6 and Stephens 9 wells are all currently producing O&G wells that correlate with occurrence of the upper "A" Zone Viola facies, which predominantly consists of well-developed rhombic dolomite with intercrystalline and fracture porosity. In contrast, the nearby non-producing D&A wells, such as the Stephens 3 and Stephens 8 wells, typically exhibit a notable decrease in both dolomite and fabric-supporting porosity. The inconsistent presence of dolomite and porosity in the Stephens Ranch wells, is possibly due to variable dolomitization processes occurring between the adjacent "A" and "B" Zone lithofacies, combined with preferential erosion during the uppermost Viola unconformity. Based on petrographic observations, it is inferred that the underlying "B" Zone formed via a "Dorag" mixing-zone type model for dolomitization. Dolomitization via this mechanism characteristically inhibits matrix-development of intercrystalline porosity (Warren, 2000). In contrast, the top "A" Zone facies is inferred to have formed via a classic model of seepage-reflux dolomitization, which is associated with an increase in Mg^{2+}, enhancing the presence of dolomite, and simultaneously increasing the pore volume with prominent fabric-supported intercrystalline porosity. The two dolomitization models may have occurred sequentially or simultaneously; nonetheless the seepage-reflux model is associated with more favorable reservoir conditions where there is a presence of dolomitized erosional remnants that were at one point in time a paleotopographic high.

Alongside the geological explanation for the unpredictable hydrocarbon production in the Morrison Northeast field, there is also geophysical data that supports this hypothesis. Based on the 3D seismic attribute analysis, the same O&G wells with a productive "A" Zone facies are represented as diagnostic thin beds with anomalously low amplitude tuning effects. In contrast,

the non-producing Stephens 3 and Stephens 8 wells both correlate to where there is an increase in the normalized amplitude and diminished instantaneous frequency. At last, these applied 3D attributes have been able to delineate stratigraphic heterogeneities and define the limits of where the top dolomitized “A” or “B” Zone facies in the Viola limestone is the most productive.

Chapter 7 – Future Work

The seismic attribute analysis in conjunction with the petrographic study of the Viola limestone in the study area has proven thus far to provide a proper workflow on correlating which zones yield higher productivity. The wells associated with higher production rates exhibit both a diagnostic rhombic dolostone facies with prominent intercrystalline and fracture porosity, along with an apparent lower amplitude anomaly and instantaneous frequency thin beds.

Fields in Kansas that are known to have unpredictable production rates should incorporate a predrilling workflow of correlating the target formation’s lithofacies to the 3D seismic facies. If the hydrocarbons in the formation of interest are not structurally trapped, then the stratigraphic heterogeneities across the field must be delineated. Knowing the lateral variations between nearby wells will not only improve understanding of the formation of interest, but will also ultimately aide in reducing the amount of dry holes that are drilled.

References

Anastasiu, N., and Dumitru-Relu, R., 2009, *Postdepositional Evolution of the Carbonate Reservoir Systems from the Moesian Platform (Romania):* University of Bucharest; AAPG Datapages, 1-11 pp.

Badiozamani, K., 1973, *The Dorag Dolomitization Model-Application to the Middle Ordovician of Wisconsin:* J. Sedim. Petrol, v. 43, 965-984 pp.

Bathurst, R.G., 1975, *Carbonate Sediments and their Diagenesis:* Elsevier, New York, 2nd ed., 321-543 pp.

Blakey, R., 2016, *Paleogeography Maps- Teaching Material Images:* Professor Emeritus, Northern Arizona University, NAU.edu.

Boggs, S., and Krinsley, D.H., 2006, *Application of Cathodoluminescence Imaging to the Study of Sedimentary Rocks*. Cambridge: Cambridge UP. 109- 117 pp.

Bornemann, E., Doveton J.H., and St. Clair, P.N., 1982, *Lithofacies Analysis of the Viola Limestone in South-central Kansas:* Kansas Geol. Survey, Petrophysical Series 3, 50 pp.

Carlson, M.P., and Newell, K.D.,1997, *Stratigraphy and Petroleum Potential of the Simpson and Viola (Ordovician) in Kansas and Nebraska. Simpson and Viola Groups, in the Southern Midcontinent, 1994 Symposium:* Oklahoma Geol. Society, 58-65 pp.

Cole, V.B., 1975, *Subsurface Ordovician-Cambrian Rocks in Kansas:* Kansas Geological Survey Subsurface Geol. Series 2, p. 18.

Cone, M. P., and Kersey, D.G., 1992, *Porosity Part 5: Laboratory Methods:* AAPG Special Volumes ME10, 204-09 pp.

Green, M.W., and Fairer, G.M., 1995, *Geologic Overview of Clark County, Kansas:* 1U.S. Geol.Survey. 1-18 pp.

Harries, P. J. 2009, *Epeiric Seas: A Continental Extension of Shelf Biotas*: Encyclopedia of Life Support Systems. v. 4., 1-6 pp.

IHS Global Inc., 2012, Petra Mapping Software, Version 8.7.

Kansas Geological Survey (KGS), 2016, <http://www.kgs.ku.edu> Accessed, 2014-2016.

Longman, M.W., 1981, *Carbonate Diagenesis as a Control on Stratigraphic Traps*: AAPG Education Course Note Series 21, 159 pp.

Merriam, D.F., 1963, *KGS--Geologic History of Kansas—Tectonic Framework.*: Kansas Geol. Survey Bulletin 162, 317 pp.

Machel, H.G., 2004*, Concepts and Models of Dolomitization: A Critical Reappraisal*: The Geol. Society of London, Special Publications, 235, 7 -63 pp.

Mazzullo, S. J. 2004, *Overview of Porosity Evolution in Carbonate Reservoirs*: Search and Discovery; Kansas Geol.Society, 79, 1-19 pp.

Murray, R. C., Pray, L.C., 1965, *Dolomitization and Limestone Diagenesis, A Symposium:* Soc. Econ. Paleontologists and Mineralogists Special Publ. 13, 180 pp.

Richardson, L. J., 2013, *The Herd Viola Trend, Comanche County, Kansas: AAPG Mid-Continent Section Meeting* 20220th ser., 1-32 pp.

Shinogle, H. 2015, Personal interview.

Sloss, L. L., 1987, *Sedimentary Cover: North American Craton: U.S.*: Boulder, CO: Geol Society of America. DNAG, Geology of North America, v. 2. 506 pp.

St. Clair, P. N., 1985, *Core studies of the Viola Limestone in Barber and Pratt counties, south-central Kansas; in, Core Studies in Kansas; Sedimentology and Diagenesis of Economically Important Rock Strata in Kansas, W. L. Watney, J. H. Doveton, and A. W. Walton, comps.:* Kansas Geological Survey, Subsurface Geology Series 6, 8-16 pp.

Syed, A. A., Clark W.J., Moore W.R., and Dribus, J.R., 2010, *Diagenesis and Reservoir Quality:* (Oilfield Review), Schlumberger, n. 2, 14-27 pp.

Vaziri, S. H., Fursich, F.T., and Kohansal-Ghadimvand, N., 2012, *Facies Analysis and Depositional Environments of the Upper Cretaceous Sadr Unit in the Nakhlak Area, Central Iran*: Scielo Publication. n. 2, v. 29, 385- 397 pp.

Vohs, A B., 2016, *3D seismic attributes analysis in reservoir characterization: The Morrison NE field & Morrison field, Clark County Kansas*, M.S. Thesis, Kansas State University, 91 pp.

Warren, J.K., 2000, *Dolomite: Occurrence, Evolution and Economically Important Associations*: Earth Science Reviews, no. 1-3, p. 1-81.

Welch, C.L., 2001, *Petrography and Geochemistry of Dolomites in the Lower Cretaceous Edwards Formation, Taylor County, Texas:* M.S. Thesis, *Texas* Tech University, 129 pp

Raef, A., Totten, M., Vohs, A., and Linares, A., in press, *3D seismic attributes and lithofacies analysis in reservoir characterization: Morrison NE Field and Morrison Field, Clark County, KS:* Journal of Applied Geophysics.

Appendix A– Elemental Maps

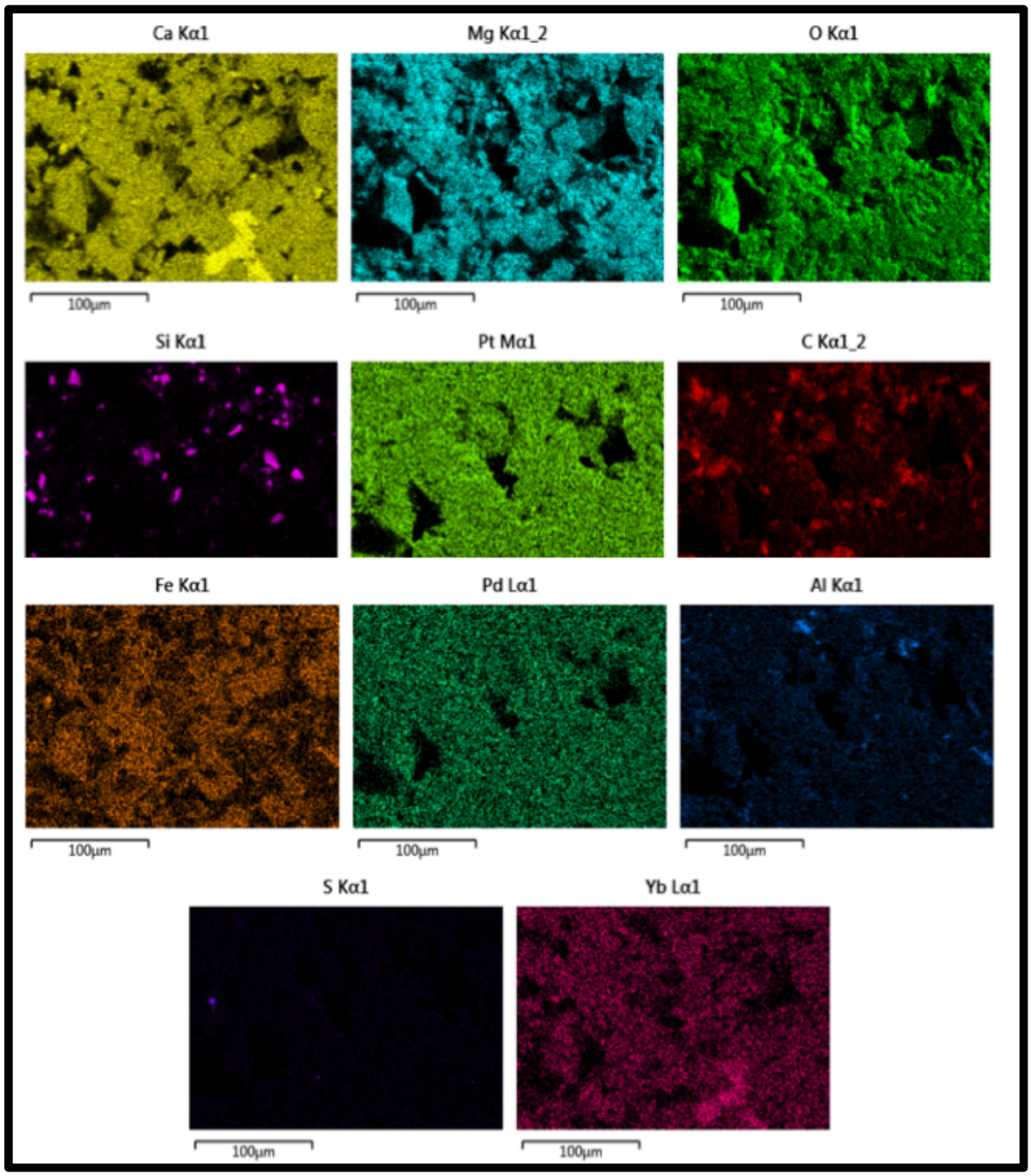

Figure A-1. Example FEI Versa DualBeam SEM image (Stephens 6), with the corresponding elemental maps that break down the individual elements that make up the sampled area.

Appendix B– Extra Thin Section Images

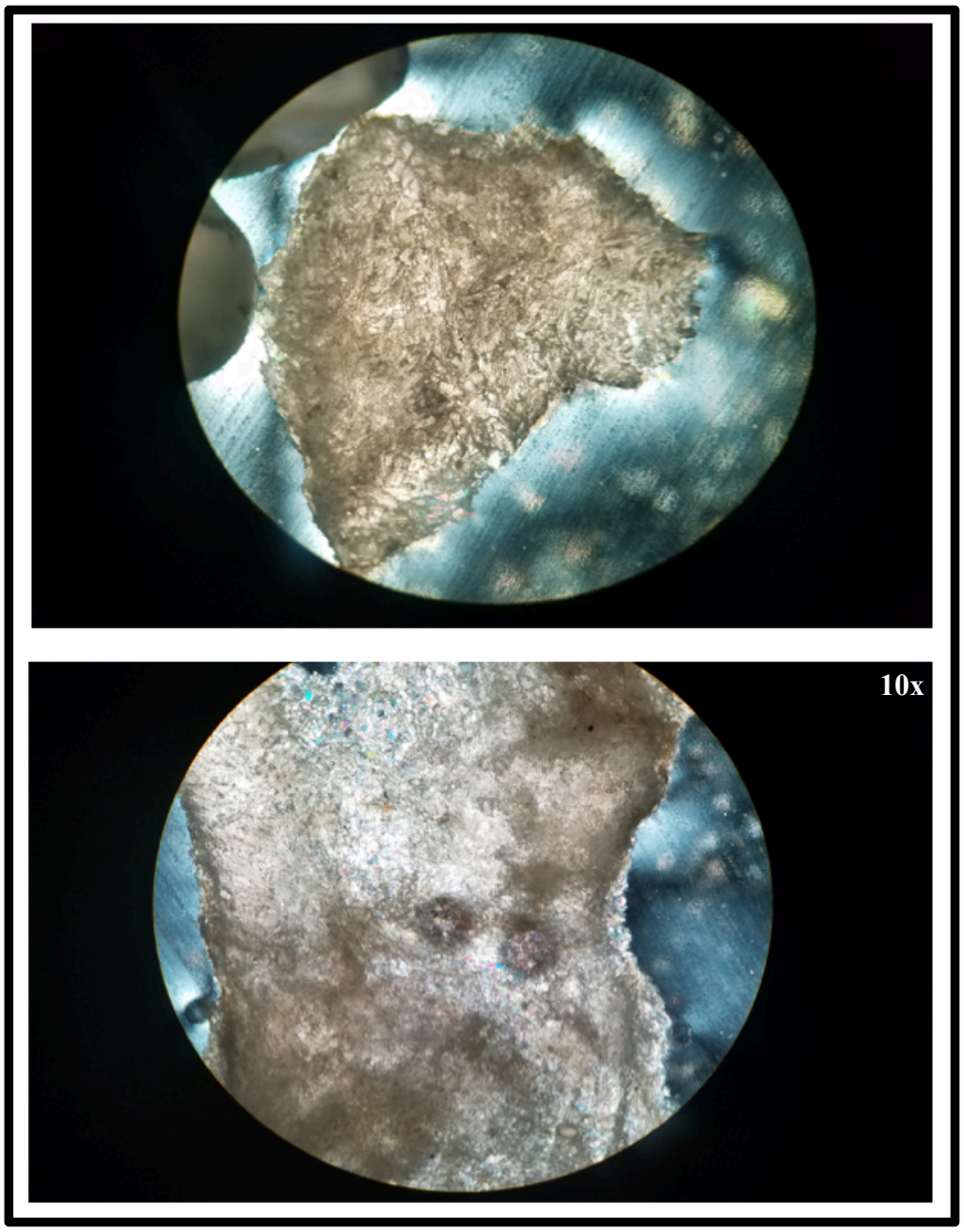

Figure B-1. Optical PPL thin section image of anhydrite grains present in Stephens 6 well.